geosciences

MDPI

Article

Sedimentology and Stratigraphy of an Upper Permian Sedimentary Succession: Northern Sydney Basin, Southeastern Australia

Sean Melehan [1], Chrysanthos Botziolis [2], Angelos G. Maravelis [3,*], Octavian Catuneanu [4], Kevin Ruming [5], Erin Holmes [5] and William J. Collins [6]

1 School of Environmental and Life Sciences, University of Newcastle, Callaghan, NSW 2308, Australia; Sean.Melehan@uon.edu.au
2 Laboratory of Sedimentology, Department of Geology, University of Patras, 26504 Rion, Greece; Ch.Bot@outlook.com
3 Department of Geology, Aristotle University of Thessaloniki, 54124 Thessaloniki, Greece
4 Department of Earth and Atmospheric Sciences, University of Alberta, 1-26 Earth Sciences Building, Edmonton, AB T6G 2E3, Canada; octavian@ualberta.ca
5 Department of Industry, Division of Resources and Energy, Geological Survey of NSW, Maitland, NSW 2320, Australia; kevin.ruming@planning.nsw.gov.au (K.R.); erin.holmes@planning.nsw.gov.au (E.H.)
6 Department of Applied Geology, The Institute for Geoscience Research (TIGeR), Curtin University, GPO Box U1987, Perth, WA 6845, Australia; William.Collins@curtin.edu.au
* Correspondence: author: angmar@geo.auth.gr

check for updates

Citation: Melehan, S.; Botziolis, C.; Maravelis, A.G.; Catuneanu, O.; Ruming, K.; Holmes, E.; Collins, W.J. Sedimentology and Stratigraphy of an Upper Permian Sedimentary Succession: Northern Sydney Basin, Southeastern Australia. *Geosciences* **2021**, *11*, 273. https://doi.org/10.3390/geosciences11070273

Academic Editors: Luca Mao and Jesus Martinez-Frias

Received: 13 April 2021
Accepted: 25 June 2021
Published: 29 June 2021

Publisher's Note: MDPI stays neutral with regard to jurisdictional claims in published maps and institutional affiliations.

Copyright: © 2021 by the authors. Licensee MDPI, Basel, Switzerland. This article is an open access article distributed under the terms and conditions of the Creative Commons Attribution (CC BY) license (https://creativecommons.org/licenses/by/4.0/).

Abstract: This study integrates sedimentological and stratigraphic insights into the Upper Permian sedimentary rocks of the Wittingham, Tomago and Newcastle Coal Measures in the Northern Sydney Basin, Australia. Facies analysis documented fifteen facies that belong to seven facies associations. These facies associations correspond to different depositional environments and sub-environments including prodelta, delta-front, upper, lower delta-plain and fluvial. The stratigraphic development points to a shallowing upward trend and is reflected with fluvial deposits sitting on top of the deltaic deposits. The fluvio-deltaic contact is represented by an unconformity and displays an upward increase in sediment caliber. The delta front is mainly controlled by wave, storms- and/or river currents, even though the contribution of tides also occurs in the form of sedimentary structures that suggest tidal influence. In contrast, prodelta and delta-plain are significantly modulated by tidal currents. The impact of tides in the delta plain is fading away upward and therefore, the upper delta plain is much less impacted compared to the lower delta plain. The low abundance of wave ripples suggests that the wave action was not very important in the delta plain. Steep topographic gradients and increased sediment input are suggested, based on the limited or absent evidence of tides in the fluvial realm, related to the growing New England Orogen. In sequence stratigraphic terms, the deltaic system accumulated during highstand normal regression, while the deposition of the overlying fluvial system occurred during lowstand normal regression. The two systems are separated by a subaerial unconformity developed during an intervening forced regression. Short periods of transgression are inferred from the presence of higher frequency cycles in the delta-front.

Keywords: core analysis; stratigraphic correlation; permian; sydney basin; Australia

1. Introduction

Marginal-marine depositional environments (deltas-estuaries) have great economic potential and there is a wealth in the literature of papers that deal with the development of these deposits (e.g., [1–4]). Some notable examples of such deltaic systems that have been studied in relation to facies analysis and sequence stratigraphy exist (e.g., [5–7]). Deltaic systems are areas where different depositional processes (fluvial, tidal, wave and storm currents) interact, giving rise to composite depositional pattern that is additionally

governed by tectonics and relative sea-level changes [8,9]. Deltas are governed by fluvial processes but are modulated by tidal and wave/storm currents [10,11]. The passage from continental (fluvial) to marginal-marine (estuarine) realm, and the switchover from delta-plain to fluvial sedimentation in fluvio-deltaic systems have been documented in the literature [4,6,11–14]. In some cases, the latter transition includes development of fluvial deposits that are modulated by tides [6] whereas in some instances, the fluvio-deltaic boundary is held with sharp evolution from delta-plain to fluvial deposits [4,11].

The Sydney Basin represents a Permo-Triassic sedimentary basin in eastern Australia that hosts several thick coal-prone deposits, associated with deltaic settings (Figure 1). The Sydney Basin and nearby regions (e.g., Myall Trough) have attracted both academic and industry interest (e.g., [15–20]). Improving the extraction of oil/gas reserves from such deltaic systems is dependent on detailed litho-stratigraphic correlations combined with precise spatial distribution parameters of economic resources, and has resulted in numerous studies (e.g., [15–27]).

Despite the research conducted in the basin [28–37], the definition of the sedimentary facies and related depositional environments based on comprehensive sedimentological analysis is still very rare (e.g., [4,35]). The northern edge of the Sydney Basin (referred hereafter as NSB) offers a case study to build on the existing knowledge about the regional facies model development. This study focuses on the Upper Permian Wittingham, Tomago and Newcastle Coal Measures that are widespread in the NSB (Figures 1 and 2). CA-IDTIMS results document that the studied succession is of Late Permian in age (Wittingham Coal Measures: 257.43 $\pm$ 0.06 to 257.04 $\pm$ 0.06 Ma [38], Newcastle Coal Measures: 255.65 $\pm$ 0.08 to 255.08 $\pm$ 0.09 Ma [39], 255.02 $\pm$ 0.03 Ma) [38]. The Tomago Coal Measures are regarded an equivalent of the Hunter Coalfields Wittingham Coal Measures [30]. The depositional environments change up-sequence from pro-delta to a coarser delta front [28]. Marginal marine conditions returned, and in conjunction with the limited sedimentation for long period, resulted in the formation of coal-bearing swamps [28]. Following evidence of marine fauna and ice rafting from erratics points to the return of a fully offshore marine environment [28].

The basal two-thirds of the Newcastle Coal Measures have been regarded as deposits by meandering rivers, whereas the upper third has been interpreted as braided river deposits [28,30]. Freshwater supplied by the river system influenced coal deposits, in contrast to the marine-influenced coal of the Tomago Measures. The Newcastle Coal Measures include both regressive and transgressive deposits [31,32]. Contrasting scenarios exist regarding the regional stratigraphic evolution. These scenarios include: (a) the existence of a regional erosional surface, which defines the change from the underlying deltaic deposits to the overlying fluvial deposits [4,39] and (b) a more complicated stratigraphic evolution, consisting of several erosional surfaces that occur at different stratigraphic levels, proposing several repetitions of deltaic and coastal deposits [35]. However, recently obtained CA-IDTIMS results document that the proposed by [35] stratigraphy is repetitive and does not reflect the actual stratigraphic record [39]. The dating results fit well with the proposed sequence-stratigraphic scenario of [4] and indicate the development of a regressive fluvio-deltaic system, rather than multiple repetitions of deltaic and coastal plain deposits (see [4,39] for further discussions).

This study employs more sedimentological evidence to shed light on the involved depositional environments and sub-environments, as well as to document the sequence-stratigraphic framework.

This research is applied to a sedimentary succession that is typified by an upward shallowing tendency from prodelta and delta-front, to delta-plain and fluvial deposits, indicating the gradual fill of the NSB. Sedimentological and stratigraphic results were employed to define the dominant sedimentary processes that governed the NSB during the deposition of the studied sedimentary rocks, as well as the stratigraphic evolution of the basin. The results of this research will assist to the knowledge of the response of the depositional environments across the fluvio-deltaic boundary, offering conclusions

regarding the type (gradual vs abrupt) of this transition. This research establishes tighter litho-stratigraphic correlations between the economically viable resources in the NSB.

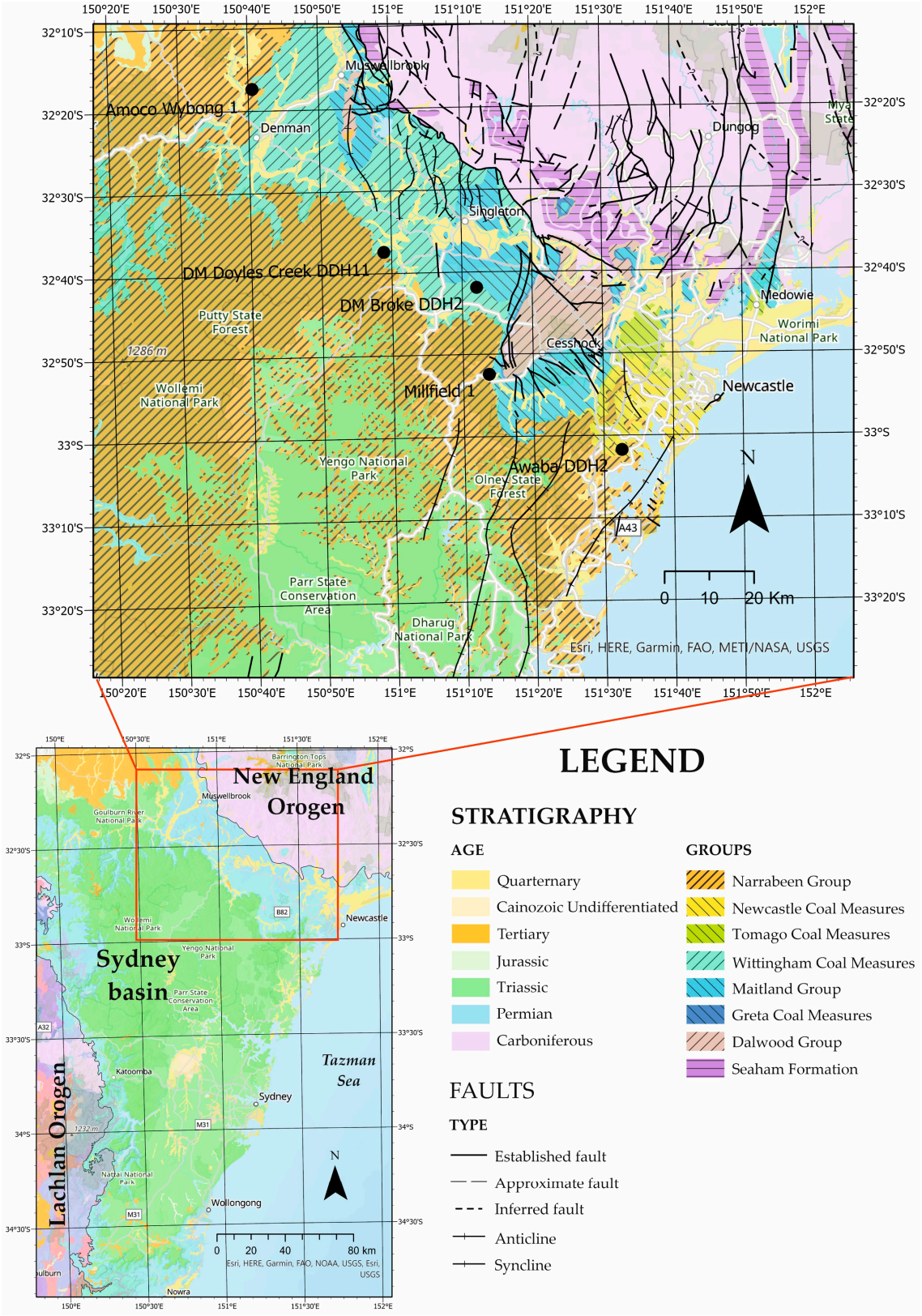


Figure 1. Geological map illustrating the Sydney Basin, bounded by the New England and Lachlan Orogens (modified from Geological Survey of NSW).

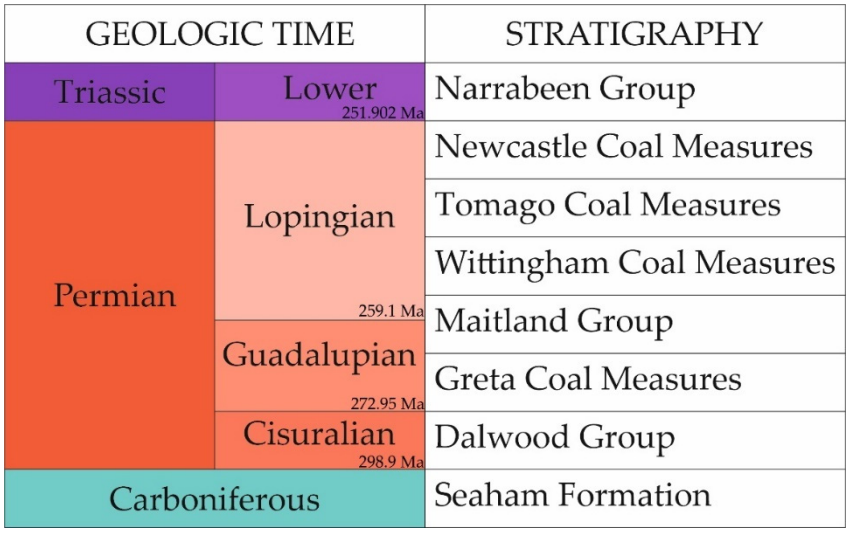


Figure 2. Carboniferous to Permian stratigraphic column of the Northern Sydney Basin (modified from [40,41]).

2. Geological Setting

The Sydney Basin (Figure 1) was developed during the Early Permian to Middle Triassic and forms part of the larger Bowen-Gunnedah-Sydney Basin [42]. The Bowen-Gunnedah-Sydney Basin is an NNW trending, asymmetric retroarc foreland that is bounded by the Lachlan Orogen to the southwest and the New England Orogen to the northeast [42]. The basement of the Sydney Basin is constituted of Ordovician, Silurian and Devonian metamorphic rocks, as along with Devonian and Carboniferous plutons [43,44]. The geodynamic framework suggests the presence of a magmatic arc province that migrated as a result of the combined extensional and strike-slip tectonic forces [45]. This process took place during the Late Carboniferous to Early Permian and brought about intrusion of S-type granitoids and ignimbrites in the New England Orogen [45]. During the Late Permian, the region is characterized by the uplift of the New England Orogen that has been ascribed to the beginning of the Hunter-Bowen Orogeny [46,47]. This process was most likely assisted by right-lateral tectonics that affected the onset of orogenesis [48].

The geodynamic evolution of the Sydney Basin is complicated and displays periods of both extension and compression. The Early Permian is characterized by extension and erosion of the Lachlan and New England Orogens [49]. Further, the temperature drop in the magmatic arc was responsible for basin subsidence [50]. During this time, extensive stretching of the crust that was related to the eastwards migration of the subduction zone is documented by the development of the East Australian Rift System [51–54]. This system is of great aerial extent and is present in northern Queensland, New South Wales and Tasmania [51–54]. This rifting brought about the input of sea water in the Sydney Basin, leading to the development of both continental and shallow-marine depositional environments [55–57]. The extensional tectonic regime (continental rift) was followed by regional contraction (foreland basin) and westward thrusting during the Late Permian, as indicated by the structural analysis [46,49,58].

In the NSB, the New England Orogen is considered as the major sediment contributor [59]. The Late Permian growth of the New England Orogen and associated shoreline regression favored the accumulation of continental and marginal marine sedimentary rocks that include the economically important coal deposits of the Newcastle Coal Measures [60–63]. Additional Late Permian-Early Triassic regional compression resulted in supplementary deformation and thrusting of the Tamworth Terrane onto the Bowen-Gunnedah-Sydney Basin, enhancing the deposition of alluvial sedimentary rocks [64,65]. The ceasing of sediment deposition in the Sydney Basin took place during the Middle to

Late Triassic [28] because of crustal shortening associated to the westward migration of the thrust systems.

3. Materials and Methods

Basin analysis requires the accurate interpretation of the environments and sub-environments of deposition, and facies analysis is the key for the reconstruction of the stratigraphic evolution in sediment depocenters. Facies analysis has been employed to unravel the depositional conditions to both non-marine and marine deposits (e.g., [20,66,67]), and to present differences between extensional and compressional regimes [68,69].

The studied succession is composed of Wittingham, Tomago and Newcastle Coal Measures. The research area was defined along a 120 km line trending approximately northwest to southeast across the Upper Permian Newcastle and Hunter Coalfields (Figure 1). Five cores were selected to create a cross-sectional area designed to enable the correlation of depositional environments in this area. Cores range in depth from 314 m to 1097 m and were accessed through the Department of Primary Industry's Wyee and Londonderry Core Libraries. Cores have been drilled between 1966 and 1996 by both private and State bodies.

Facies analysis was based on the identification of sedimentological features, such as lithology, sedimentary structures and texture that were acquired by detailed log descriptions. Facies characteristics were the basis for the determination of facies associations, which in turn allowed the depositional environments to be revealed. Core-based analysis permitted the identification of important marker horizons and stratigraphic surfaces in the NSB, enhancing correlations throughout the succession. The stratigraphic cross-sections provided information about the aerial and temporal distribution of the facies associations, and the temporal changes in the environments of deposition revealed the stratigraphic evolution. The interpretation of facies analysis prompted the identification of sequence-stratigraphic surfaces, which in turn bolstered conclusions about the regional sequence stratigraphic framework.

4. Sedimentary Facies and Facies Associations

In the examined succession, 15 depositional facies have been distinguished (F1–F15) and they are the building blocks of seven facies associations (FA1–FA7). The definition of facies associations is based on the facies combinations, the prevalent depositional processes responsible, and the type (erosional vs. gradual) and stratigraphic location of the principal bounding surfaces. A summary of the diagnostic features that are preserved in the sedimentary facies is illustrated in Table 1.

Table 1. A summary of facies and facies associations including sedimentary structure descriptions, depositional processes involved and depositional interpretations.

Facies	Sedimentary Structures	Depositional Process	Interpretation	Appearance
F1: Matrix- to clast-supported conglomerate	Structureless with occasional reverse to normal grading.	High energy unidirectional traction currents; weathering of source rock.	Fluvial channel created by high-flow bedload transport.	FA1, FA2
F2: Cross-stratified conglomerate	Conglomerated planar cross-stratification and trough cross-stratification	High energy traction currents; weathering of source rock.	Migration of 2D and 3D gravelly dunes in lower flow regime of tidally influenced channels.	FA1, FA2
F3: Structureless sandstone	Unstratified	Rapid suspension fallout.	Suspension deposition during flood events.	FA1, FA2, FA3, FA4, FA6

Table 1. *Cont.*

Facies	Sedimentary Structures	Depositional Process	Interpretation	Appearance
F4: Trough cross-bedded sandstone	Trough cross-stratification, commonly with mud drapes.	Unidirectional migration of 3D sand dunes.	Sand transportation in tidally influenced channels.	FA1, FA2, FA3, FA6
F5: Planar cross-stratified sandstone	Cross-stratified, commonly in sets, occasional mud drapes.	Mid to high energy, unidirectional traction sedimentation.	Migration of straight-crested sand dunes within tidally influenced channels.	FA1, FA2, FA3, FA6, FA7
F6: Parallel-laminated sandstone	Parallel lamination with occasional superimposed ripples. Rare mud drapes.	Low to mid energy, unidirectional traction sedimentation.	Planar bed deposition near or at the upper flow regime.	FA1, FA2, FA3, FA4, FA6, FA7
F7: Ripple cross-laminated sandstone	Asymmetrical ripples; frequent mud drapes.	Unidirectional traction sedimentation.	Migration of complex dunes in a tidally influenced sub-environment.	FA3, FA4, FA7
F8: Compound cross-stratified sandstone	Cross-stratification, reactivation surfaces and amalgamated surfaces; rare mud drapes	Low energy, unidirectional traction sedimentation.	Migration of weak currents in a tidally influenced depositional sub-environment.	FA1, FA2, FA3
F9: Hummocky and swaley cross-stratified sandstone	Concave and convex laminae structures over planar laminations.	Oscillatory wave motion in high-energy regimes.	Sandy infilling of scours created by storm-related events.	FA6, FA7
F10: Contorted sandstone	Overturned, folded, or disrupted cross-stratification.	Traction sedimentation and high sedimentation loading.	Deformation caused because of vertical shear forces.	FA2, FA3,
F11: Heterolithic bedding	Wavy, flaser and lenticular horizontal laminations. Occasional mud drapes.	High to low energy tidal currents and slack water suspension fallout.	Bedload transport in lower to upper tidal flats or channels in low flow regimes.	FA2, FA3, FA4, FA5, FA6, FA7
F12: Structureless mudstone	Massive, with occasional weak parallel laminations.	Suspension sedimentation.	Deposition in slack water depositional environment.	FA1, FA2, FA3, FA4, FA5, FA7
F13: Parallel-laminated mudstone	Thin horizontal laminations, often with horizontal sandstone interbeds.	Unidirectional traction and suspension sedimentation.	Suspension sedimentation interrupted by storm-related events.	FA1, FA2, FA3, FA4, FA5, FA7
F14: Ripple cross-laminated mudstone	Fine- to medium-grained sandstone, including mud laminae or mud drapes.	Asymmetrically ripple cross lamination. Common mud drapes.	Migration of complex ripples in a tidally influenced environment	FA1, FA3, FA4, FA7
F15: Bioturbated mudstone	Horizontal laminations; sedimentary structures obliterated by high degree bioturbation in places.	Suspension sedimentation.	Preservation of trace fossils in high-nutrient slack water environment.	FA3

4.1. Facies Association FA1: Fluvial Channels

4.1.1. Description

This facies associations is approximately 50–200 m thick (Amoco Wybong and Millfield wells respectively) and is dominated by conglomerate, followed by sandstone (Figure 3A).

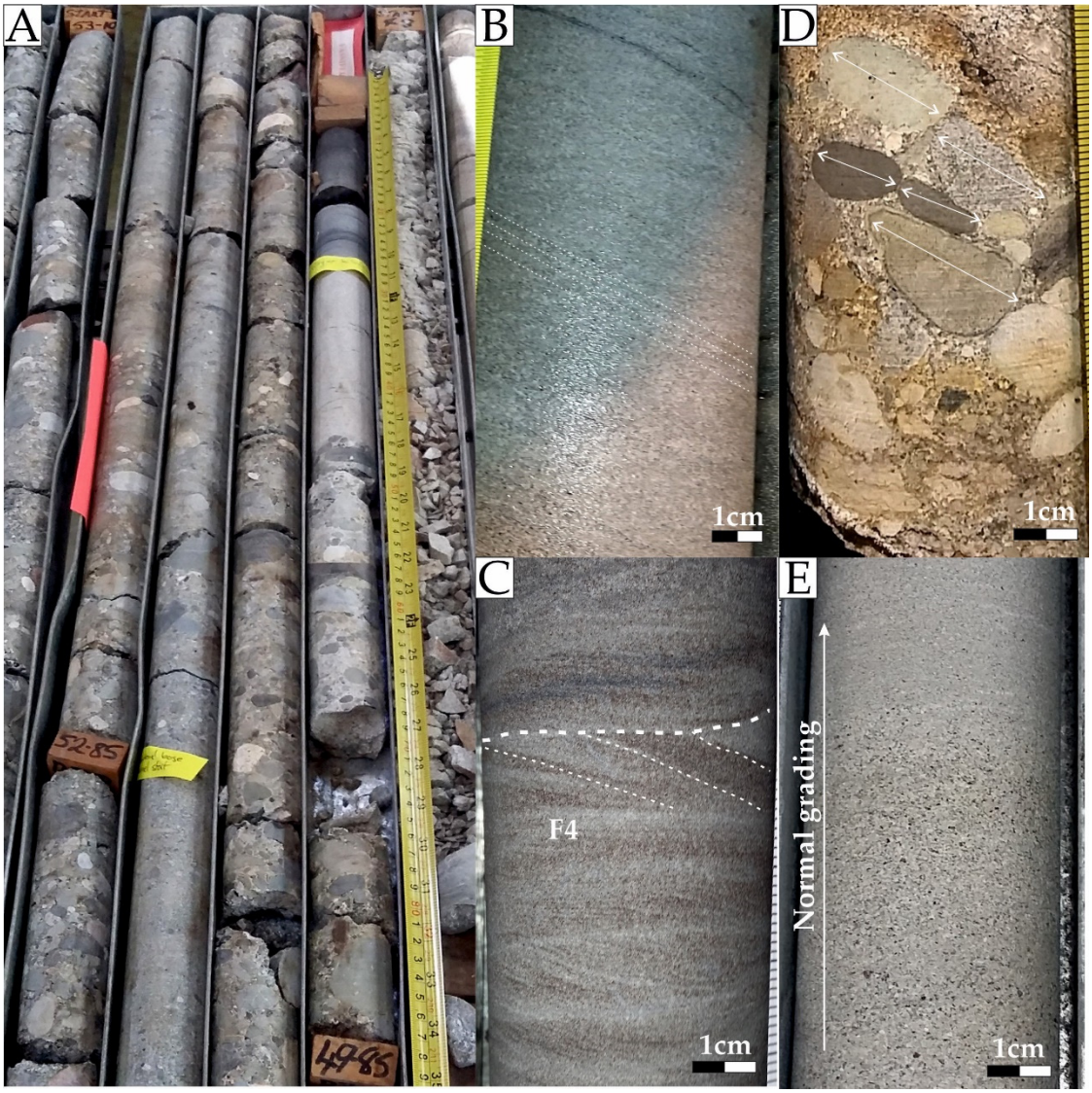


Figure 3. Core photographs illustrating sedimentological characteristics of the FA1 (fluvial channels). (**A**) Clast to matrix-supported conglomerate, followed by structureless sandstone. Note the upward decrease in the grain-size that reflects the progressive reduction of the river strength and migration of the fluvial channels. (**B**) Planar cross-bedded sandstone. Note that the cross-beds are sometimes filled with mudstone. (**C**) Co-sets of trough-cross-laminated sandstone separated by low angle bounding surfaces. (**D**) Clast-supported conglomerate exhibiting clast imbrication. (**E**) Normally-graded sandstone.

Conglomerate is matrix- to clast-supported (F1) and cross-stratified (F2), whereas sandstone is mainly structureless (F3), trough cross-bedded (F4), planar cross-bedded (F5) and parallel-laminated (F6) (Figure 3B,C). Conglomerate sometimes exhibits clast imbrication (Figure 3D). Compound cross-stratified sandstone (F8) occurs but it is far less abundant. Transported organic debris is occasionally scattered either throughout the finer-grained beds (F4, F5 and F8), or just above their bases and may occasionally develop very crude horizontal stratification. F4 and F5 usually overlie F3, typically occur as co-sets that are 0.25 m to 2.5 m thick and are made up of two to eight individual sets. F8 ranges in thickness from 0.2 m to 3.5 m and is either preserved as individual sets or as thicker co-sets. Floating pebbles of sedimentary and igneous origin are observed in cross-beds and laminations. Mudstone is not common and occurs between medium- to thin-bedded sandstone (0.1–0.3 m). Mudstone is structureless (F12), however rare, horizontally laminated (F13) mudstone beds are present (Figure 3A). This FA portrays a general finning upward trend, from a basal conglomeratic part (F1 and F2) to a sandier

upper part (F3 to F6) and is characterized by the scarce presence of fine-grained deposits (F12, F13 and F14). The basal, conglomeratic part is thick-bedded (1–3 m) and almost entirely amalgamated, with clasts ranging from 3 mm to 80 mm (Figure 3D). However, several beds are dominated by conglomerate clasts of 10 mm to 25 mm in diameter. All clasts are of medium to high sphericity and of low to moderate angularity. The upper part is composed of thick-bedded (0.8–1.5 m) and amalgamated sandstone units and contains less frequently conglomeratic beds. These beds are generally thinner-bedded (up to 1 m) and finer-grained, compared to their basal equivalents. FA1 displays usually erosional basal contacts with the underlying sediments, however sharp basal contact also exists. This contact usually truncates finer-grained overbank deposits (FA4).

4.1.2. Interpretation

FA1 is interpreted as braided fluvial channels. the presence of conglomeratic packages limited at the base by erosional concave-up surfaces (5th order surface of Miall, [70]) supports this conclusion. The clast-supported conglomerate and sandstone with floating larger clasts can be ascribed to bedload deposition from stream flows [71]. The fluctuations between matrix- and clast-supported conglomerate is most likely related to variations in the flow energy [72]. Furthermore, the prevalence of sandstone beds that are dominated by unidirectional planar and trough cross-stratification and with a well-developed fining upward trend further supports this braided-river origin of the FA1 [71,73,74]. Horizontal stratification of pebbles is a characteristic feature of deposition on horizontal or near-horizontal surfaces and are associated with braided fluvial bars or channels [71]. Thin-bedded conglomerate below planar (F4) and trough cross-bedded sandstone (F5) could be associated to channel lag deposits and correspond to sediment transported by the flow during high-energy conditions. The absence of fine-grained deposits, combined with the amalgamated nature of this FA indicates that procedures, such as cut-and-fill, were active and is consistent with low-sinuosity channels, probably of braided type [75]. The general upward fining motif is most likely due to falling flood stage or to gradual abandonment of fluvial channels [73,76].

4.2. Facies Association FA2: Weakly Tidally-Influenced Channels (Upper Delta-Plain)

4.2.1. Description

FA2 resembles FA1 and is approximately 10–50 m thick (Broke and Doyles Creek wells respectively). It forms thick sedimentary packages (1 to 15 m thick). It is composed of matrix- to clast-supported (F1) and cross-stratified (F2) conglomerate, as well as structureless (F3), trough cross-bedded (F4), planar cross-bedded (F5) and parallel-laminated (F6) sandstone (Figure 4A).



Figure 4. Core photographs illustrating sedimentological characteristics of the FA2 (upper delta-plain channels). (**A**) Clast to matrix-supported conglomerate, interbedded with structureless sandstone. (**B**) Repetitions of structureless to parallel-laminated sandstone and mudstone. (**C**) Transported coal debris in FA2. (**D**) Normally- to reverse-graded sandstone bed. (**E**) Erosional contact of FA2 with the underlying fine-grained deposits. Note the loading of sandy material in the underlying mudstone.

Compound cross-stratified sandstone (F8) also occurs but it is far less abundant. This FA also includes convoluted sandstone (F10) and heterolithic bedding (F11), which is principally represented by sand-prone units (flaser bedding) (Figure 4B). FA2 contains transported coal debris (Figure 4C). Finer-grained sediments are more common than FA1, but they are still very rare. When present, they correspond to structureless and/or parallel-laminated mudstone (F12 and F13). The sandy units are composed of fine- to coarse-grained, poorly to well-sorted sandstone. The sandstone beds are normally- to reverse-graded and may occasionally include pebbly layers (Figure 4D). Internally, erosional surfaces between sandstone beds are common. Mud drapes occur sparsely throughout FA2, and are preserved within F4, F5, F6, F10 and F11. Occasional paired mud drapes occur, separated by thin sandstone layers. FA2 exhibits mostly sharp, but often erosional contacts with the underlying sediments, with the scour surfaces being mantled with pebbles (Figure 4E).

Similarly to FA1, FA2 displays a thinning and finning upward trend, with a conglomeratic basal part (F1 and F2) that evolves up-sequence into sandier facies (F3, F4, F5, F6, F8, F10 and F11). The most characteristic difference between FA2 and FA1 is the occurrence of mud drapes and heterolithic bedding in FA2. Compared to FA1, FA2 is also finer-grained and thinner-bedded and is more often interbedded with overbank deposits (FA4), suggesting lower degree of amalgamation.

4.2.2. Interpretation

FA2 deposits are interpreted as weakly tidally-influenced channelized deposits in an upper delta plain setting. This conclusion is made based on the: (1) thinning and fining upward trend, (2) erosionally-based units and channelized shape, (3) abundant trough cross stratification, (4) coarse-grained character and (5) occurrence of mud drapes and heterolithic bedding. Furthermore, the lack of marine fossils suggests deposition in a tidally-influenced fluvial channel [77], in places affected by the tidal currents, where the fluvial channel evolves into a tidally-influenced distributary channel [12]. The compound cross-stratified sandstone (F8) displays asymmetric ripples that climb up the lee faces of high-angle cross-strata and indicates a much stronger dominant current [78]. The presence of contorted sandstone (F10) with irregular convolute and/or highly distorted stratification is interpreted as the result of intense liquefaction and/or fluidization, most likely stemmed by overloading or slumping [79], but also due to seismic shocks [80]. The scarce development of overbanks and/or floodplains can be indicative of a channelized setting, which is of higher sinuosity compared to FA1, but still braided, and could be ascribed to higher periodicity of channel migration and/or abandonment [66].

4.3. Facies Association FA3: Tidally-Influenced Channels (Lower Delta-Plain)

4.3.1. Description

FA3 resembles FA1 and FA2 and is approximately 150–360 m thick (Broke and Millfield wells respectively). It is composed of 0.3 m to 12 m thick sandstone-prone successions but is characterized by higher mud-to-sand ratio and minor occurrence of conglomeratic beds (Figure 5A). The main sedimentary facies include structureless (F3), trough cross-bedded (F4), planar cross-bedded (F5), parallel-laminated (F6) and ripple cross-laminated (F7) sandstone, as well as heterolithic bedding (F11) (Figure 5B).

Mudstone beds are common and are represented by structureless, parallel-laminated and bioturbated mudstone (F12, F13 and F15). In contrast to FA1 and FA2, heterolithic bedding (F11) is very abundant facies in FA3 and includes a wide range of sedimentary structures, such as flaser, wavy, lenticular bedding, single and double mud drapes, tidal bundles and bi-polar current ripples (Figure 5C,D). The mud drapes are present in trough, planar and compound cross-stratified sets (F4, F5 and F8) and are often dissected into sub-angular clasts and the tidal-bundled sandstone beds are separated by clean sandstone. The foreset thickness in the tidal-bundled sandstone beds varies in places from 0.2 to 2 cm and can be rhythmic within individual sets (Figure 5E).

Similarly to FA1 and FA2, FA3 displays a thinning and fining upward trend (Figure 5A), as well as erosional to sharp contact with the underlying deposits. The fining upward trend initiates with medium- to thick-bedded (0.5–1.5 m), fine- to medium-grained sandstone units (F3, F4, F5, F6, F7 and F11) and evolves up-sequence into thin-bedded (1–10 cm), fine-grained sandstone, which is interbedded with mudstone beds (F12, F13 and F14). The basal erosional surfaces erode or truncate (1 to 7 cm) into the underlying sediments and are often marked by a pebbly layer or coarse-grained sandstone. Compared to FA1 and FA2, FA3 contains better developed overbank deposits (FA4), reflecting an even less braided character. Further, indications of tidal influence are much more common in FA3, compared to FA2.

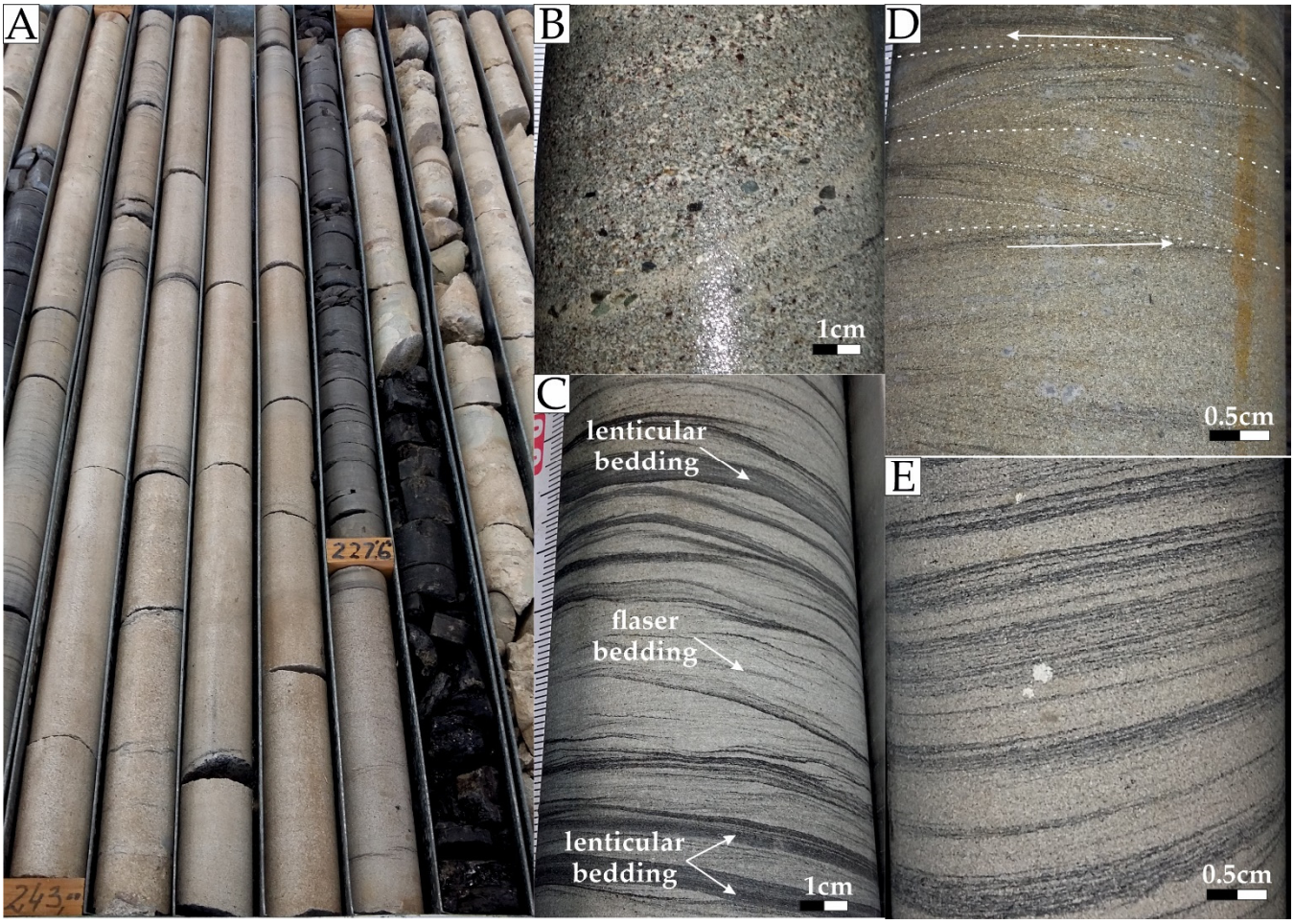


Figure 5. Core photographs illustrating sedimentological characteristics of the FA3 (lower delta-plain channels). (**A**) Structureless sandstone of FA3 that evolves into muddy deposits (FA4) and coal (FA5). The overlying conglomeratic facies correspond to upper delta-plain deposits. (**B**) Planar cross-bedded sandstone. (**C**) Heterolithic bedding with repetitions of flaser, wavy and lenticular bedding. (**D**) Bi-polar cross-bedded sandstone that suggests flow reversal during deposition. (**E**) Mud drapes with systematic variation in thickness representing deposition during neap and spring periods.

4.3.2. Interpretation

FA3 deposits correspond to channelized deposits that belong to a lower delta plain setting. Sediment deposition in a channelized setting is suggested by the presence of basal erosional contacts, abundance of sedimentary structures such as, planar and trough cross bedding, and overall fining and thinning upward trends [2,81]. The significant impact of tidal currents during deposition is supported by the abundance of sedimentary structures such as, flaser, wavy, lenticular bedding, tidal bundles, single and double mud drapes and bi-polar current ripples, and agree with a channelized setting in the lower delta plain [81]. The cyclic variation of the foreset thickness in the tidal-bundled sandstone indicates the rhythm of neap and spring tides [82,83]. The observed mud drape fragmentation can be attributed to mudstone erosion by the reversing tidal current [82]. Flow reversal is also envisaged by the bi-polar current ripples. The better developed overbanks and/or floodplains suggest a channelized setting, which is of higher sinuosity compared to FA1 and FA2 and indicate less frequent and longer channel migration and/or abandonment [66].

4.4. Facies Association FA4: Overbank Deposits

4.4.1. Description

FA4 is typically associated with FA1, FA2 and FA3 and is underlain by F12 and F13 (Figure 6A). It exhibits gradational and sharp boundaries with the underlying facies. It

comprises alterations of thin- to medium-bedded (0.1–0.3 m) sandstone and mudstone and build thin- to thick-bedded (0.3–10 m) successions (Figure 6A). The sandstone is structureless (F3), parallel (F6) and/or ripple cross-laminated (F7), whereas mudstone is structureless (F12), parallel-laminated (F13) and/or ripple cross-laminated (F14) (Figure 6B).

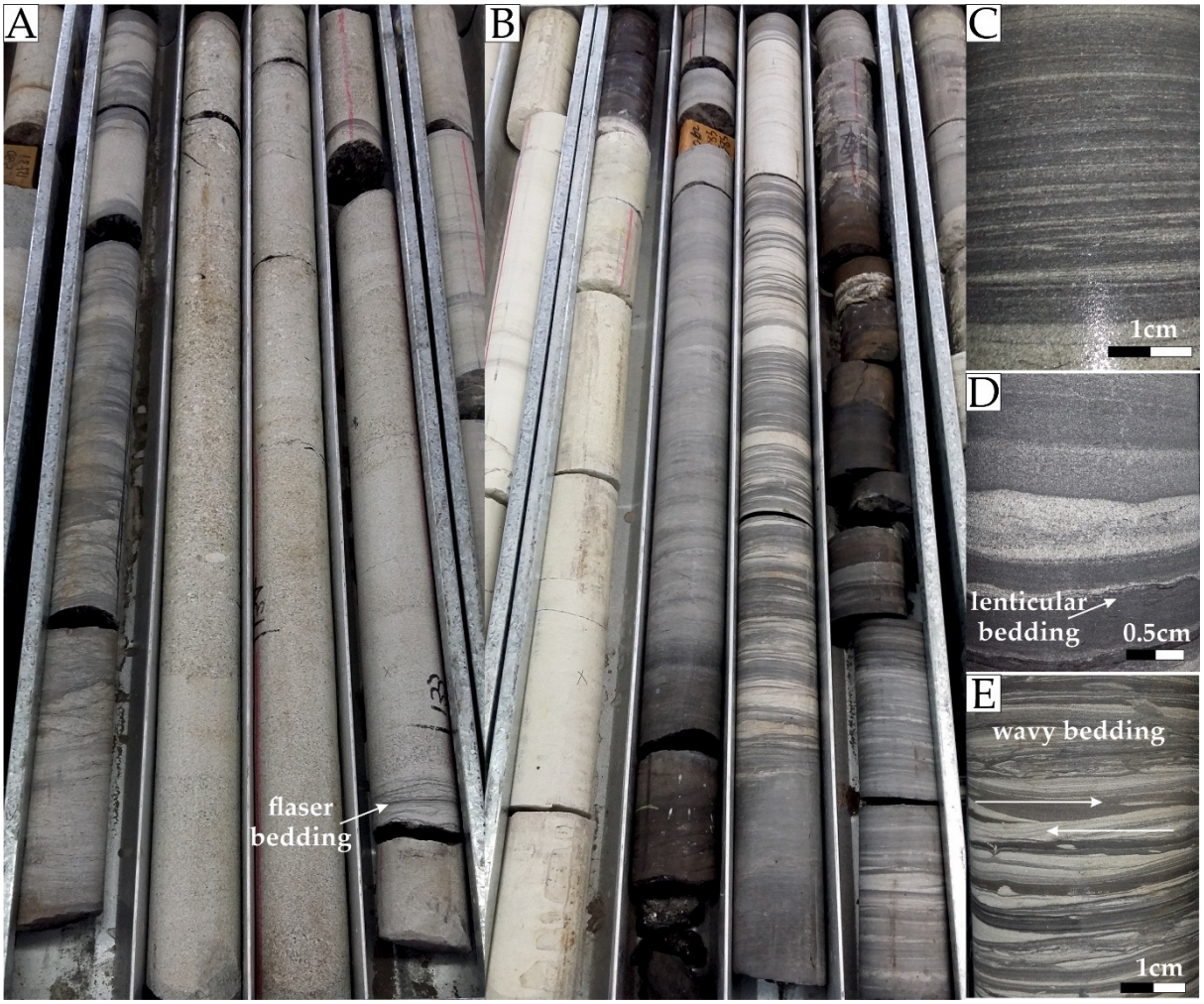


Figure 6. Core photographs illustrating sedimentological characteristics of the FA4 (overbanks). (**A**) Alternations of structureless, parallel-laminated and heterolithic bedding with structureless and/or parallel-laminated mudstone. They are underlain by structureless sandstone that belong to the lower delta-plain deposits. Note the presence of flaser bedding in the delta-plain deposits that document the presence of tidal currents during sedimentation. (**B**) Repetitions of heterolithic bedding and structureless sandstone with structureless, parallel-laminated mudstone and ripple cross-laminated mudstone. The overbank deposits evolve upward into coal-prone floodplain deposits (FA5). (**C**) Rhythmic repetitions of ripple cross-laminated sandstone with parallel laminated mudstone. (**D**,**E**) Heterolithic bedding illustrating repetitions of flaser, wavy and lenticular bedding. The opposite directed ripples within the heterolithic bedding represent the flow directions of the ebb and flood currents.

Mud drapes are often present in the ripple cross-laminated sandstone. Parallel-laminated mudstone is the most dominant facies, followed by structureless mudstone (Figure 6C). This FA develops heterolithic bedding (F11), developing sand- and mud-prone units that correspond to flaser and lenticular bedding respectively (Figure 6D). Units, containing largely equal proportions of sandstone and mudstone (wavy bedding) also exist (Figure 6D). These units include opposite-directed current ripples (Figure 6E). Often, flaser, evolves upward to wavy and finally lenticular bedding. The sandstone may exhibit flat and/or lenticular tops, whereas the bases are flat or occasionally erosional. Siderite concretions and syneresis cracks are observed in places. Coal deposits occur within FA4.

The contacts boundaries between mudstone and overlying coal are mostly sharp but are commonly gradational. FA4 is interbedded with FA2 and more commonly with FA3 in the studied succession, whereas it is thinner, rarer and sandier when interbedded with FA1.

4.4.2. Interpretation

This FA is interpreted as overbank deposits. The finer-grained character of FA4 can be attributed to sediment deposition in a low energy environment [73]. The close association of FA4 with channelized deposits (FA1, FA2 and FA3) reinforces the interpretation of an overbank or floodplain depositional sub-environment [84]. Parallel-laminated mudstone indicates sediment reworking by weak currents [6]. Heterolithic bedding is present when FA4 is interbedded with FA2 and/or FA3 deposits, suggesting tidal reworking. In such cases, the presence of coal seams, syneresis cracks and sideritic concretions suggests that some of these FA were deposited in low topographic regions, close to the distributary channels [85]. The syneresis cracks develop because of shrinkage of fine-grained sediments (mud) that results from differences in salinity or chemical conditions [86]. When FA4 is interbedded with FA1 deposits, it lacks heterolithic bedding, coal seams and syneresis cracks and is typified by reddish color, indicating sediment accumulation in the fluvial system. The decrease in frequency and thickness, in conjunction with the increase in sediment grain size of the FA4 at higher stratigraphic levels suggest augmented levels of erosion in the overbank setting [66].

4.5. Facies Association FA5: Coal-Prone Floodplain Deposits

4.5.1. Description

FA5 is made up of coal beds which can range in thickness from 5 cm to 6 m (Figures 5A and 6B). Coal is distinctively black but is sometimes interlaminated with mid-grey mudstone and white to cream tuff (Figure 6B). Lower bed boundaries are predominantly sharp but can be erosional and gradational. Upper boundaries are almost exclusively sharp and usual horizontal, although some are erosional. The underlying deposits consist of heterolithic bedding (F11), structureless (F12) and/or parallel-laminated mudstone (F13 of FA4. Often, coal deposits underlay channelized sedimentary rocks that belong to the upper and lower delta-plain.

4.5.2. Interpretation

FA5 is interpreted as having formed in reducing, anoxic conditions of little to no sedimentation. This depositional environment includes deposition and compaction of plant material in a low-energy environment. The peat mires require increased humidity and a swampy depositional environment, in which rainfall overcomes evaporation and favors the quick accumulation of organic matter [87]. The thick to very thick coal deposits in the NSB suggest long-lasting conditions that favored the formation of peat mires. In marginal marine depositional environments, coal forms because of relative sea-level rise [88]. Their stratigraphic position above the delta-plain channels (FA2, FA3) suggests lateral migration of the delta-plain channels.

4.6. Facies Association FA6: Delta Front Deposits

4.6.1. Description

FA6 is approximately 100–750 m thick (Broke and Doyles Creek wells respectively) and is associated with FA3 and FA6 deposits. In most cases, FA5 overlies FA6 and is sometimes overlain by FA3, FA4 and FA5 deposits (Figure 7A). FA6 builds sandstone-dominated bed-sets, comprising medium- to thick-bedded (0.5–2.5 m), often amalgamated sandstone beds. They are sometimes interrupted by thin- to medium mudstone beds. Conglomeratic beds also exist, but are thinner-bedded and finer-grained compared to FA1 and FA2.

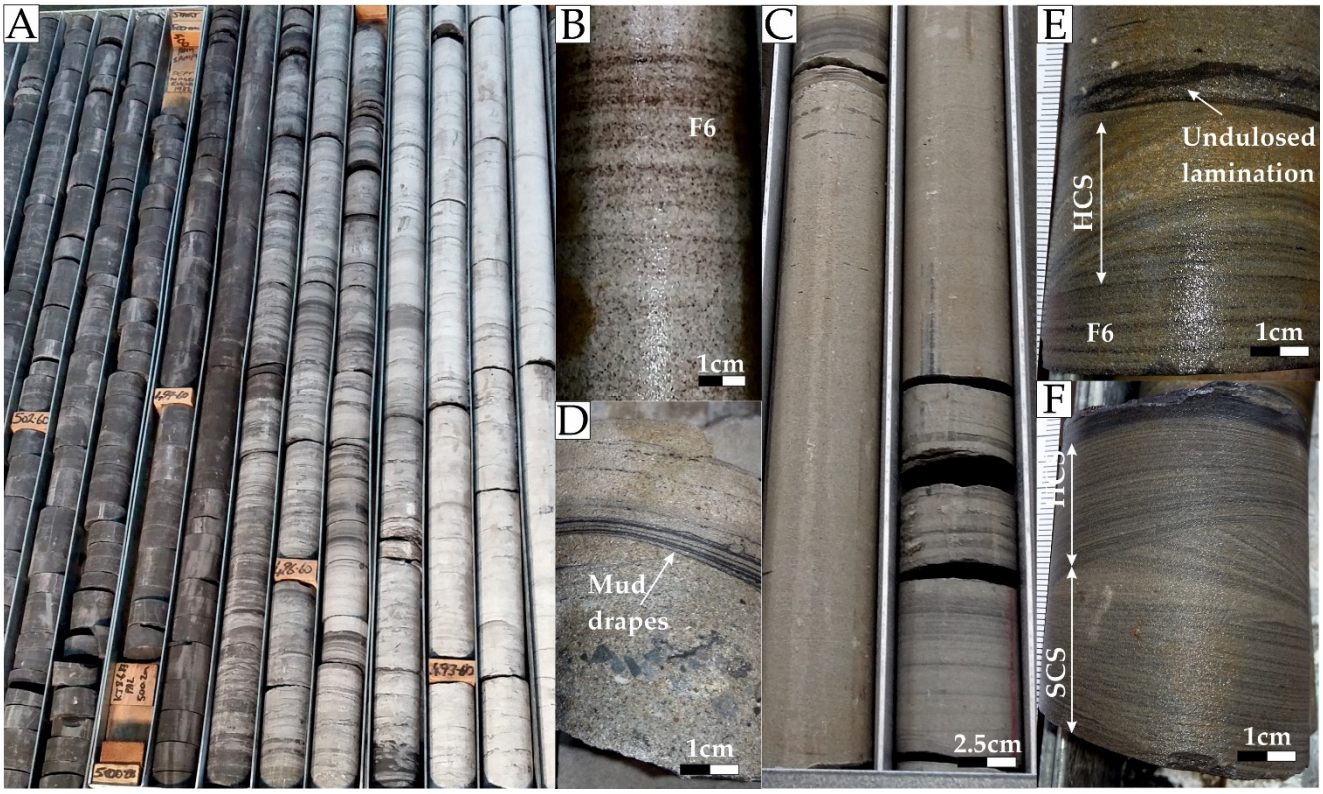


Figure 7. Core photographs illustrating sedimentological characteristics of the FA6 (delta-front). (**A**) Delta-front deposits (sand-dominated) that overlay mud-dominated deposits of the prodelta. (**B**,**C**) Structureless and parallel-laminated sandstone. (**D**) Mud and double mud drapes within FA6 that represent the depositional products of tidal currents. (**E**) HCS-sandstone with undulose lamination that is underlain by parallel-laminated unit. (**F**) SCS-sandstone that is overlain by HCS-sandstone.

The dominant sedimentary facies are structureless sandstone (F3), which is followed by trough cross-bedded (F4), planar cross-bedded (F5), horizontal to low-angle (F6) and hummocky (HCS) and swaley (SCS) cross-stratified sandstone (F9) (Figure 7B,C). Heterolithic bedding is present and mostly observed within the planar cross-bedded (F5), parallel-laminated (F6) sandstone. It is represented by flaser bedding, whereas, letricular bedding occurs scarsely in the muddier parts of FA6 (Figure 7D). Mud drapes are present within cross-laminated sandstone (Figure 7D). The HCS-sandstone often overlays parallel-laminated sandstone. The laminae forms an interval with parallel laminations that is 1–4 cm thick and underlays convex lamination (Figure 7E). The sandstone beds with SCS are characterized by concave laminations that are sometimes associated with small-scale erosional surfaces (Figure 7F). HCS-sandstone is observed on occasion at the top of sandy units, and the base of delta front deposits often exhibit trough cross-bedding. Structureless and/or parallel-laminated mudstone is not abundant, but still exists. Mud clasts occur in FA5 and are associated with erosional surfaces. Bioturbation is low.

4.6.2. Interpretation

FA6 is interpreted as the delta front part of the studied deltaic system. The presence of HCS and SCS, in conjunction with the association of FA6 with prodelta (FA7) and delta-plain (FA3, FA4 and FA5) deposits further support this conclusion. The structureless sandstone is compatible with high sedimentation rates. The thick-bedded sandstone reflects turbulence during the deposition under constant contribution of coarse detritus [89,90]. Planar and trough cross-bedded sandstone reflect deposition from unidirectional traction currents [91], suggesting the contribution of river action during deposition. Heterolithic bedding and other sedimentary structures that are associated with tidal currents (e.g.,

mud drapes) are present. However, such structures are fewer in FA6, compared to other FA's (FA3, FA4 and FA7), suggesting that the delta-front was less impacted by tides. The HCS and SCS document the impact of storms in the sedimentary succession (e.g., [92]). Wave ripples are deposited from wave currents during storm diminishing, or fair-weather conditions [93]. At the beginning of a storm, structureless or parallel-laminated sandstone reflects erosion that is followed by deposition from suspension. The presence of SCS-sandstone above scour surfaces suggest that the aggradation rates were low, preserving swales rather than hummocks [94]. The general absence of mudstone FA6 suggests high environmental energy and is compatible with a delta-front environment [95]. The low levels of bioturbation suggest that the environmental conditions did not favor the abundance of organisms and could be ascribed to an energetic depositional environment and fluvial input [96]. It could also be related to high levels of turbidity and/or low levels of salinity, indicating close relation with delta distributary mouths [96].

4.7. Facies Association FA7: Prodelta Deposits

4.7.1. Description

FA7 is 5–50 m thick (Doyles Creek well) and is associated with FA5 deposits. In most cases, FA7 underlies FA5 and overlays FA6 deposits (Figure 8A). FA7 contains significant amount of sand but is mud-dominated (Figure 8A). Therefore, thick muddy successions are commonly interrupted by thin- to medium-bedded sandstone. The bases of the sandstone beds are sharp or at times erosional, whereas the tops are planar and/or undulated. The muddy intervals can contain sandy lenses. The dominant sedimentary facies are represented by planar cross-stratified sandstone (F5), parallel-laminated sandstone (F6), ripple cross-laminated sandstone (F7), hummocky and/or swaley cross-stratified sandstone (F9), heterolithic bedding (F11), structureless (F12), parallel-laminated (F13) and ripple cross-laminated mudstone (F14) (Figure 8B,C). Conglomerate is not very common, however thin (1 to 7 cm) beds that are composed of matrix- to clast supported conglomerate and very coarse-grained sandstone are present (Figure 8D). They have been observed as either isolated pebbly layers within mudstone or at the base of coarse-grained sandstone beds. Heterolithic bedding is represented by flaser, wavy and lenticular bedding (Figure 8C,D). Syneresis cracks are often observed at the tops of mudstone beds (Figure 8E). The degree of bioturbation varies throughout the FA7, and in cases of high levels, it obliterates the primary sedimentary structures. FA7 displays a thickening and coarsening upward trend from thick, mud-dominated units to sedimentary packages that are composed of sandstone and mudstone repetitions. The lowermost muddy units comprise structureless or parallel-laminated mudstone that is interrupted by thin-bedded ripple cross-laminated sandstone and heterolithic bedding (Figure 8). The overlying repetitions are composed of parallel-laminated mudstone that are interbedded with heterolithic bedding, structureless, parallel and/or ripple cross-laminated sandstone.

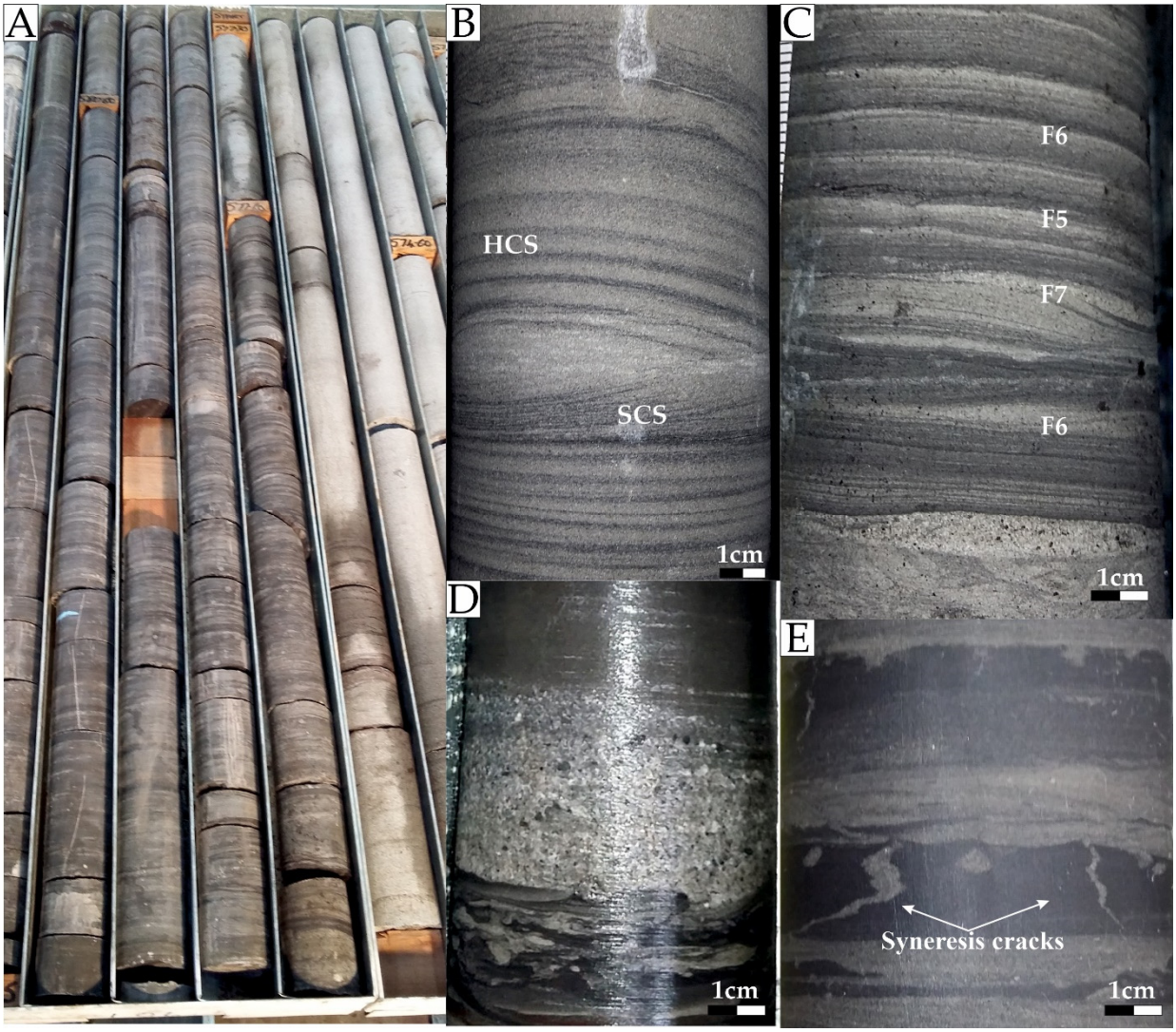


Figure 8. Core photographs illustrating sedimentological characteristics of the FA7 (prodelta). (**A**) Prodelta deposits that are overlain by delta-front deposits (FA6). (**B**) SCS-sandstone that is overlain by HCS-sandstone documenting the impact of storm currents during sedimentation. (**C**) Repetitions ripple cross-laminated sandstone and mudstone with parallel and structureless mudstone, forming heterolithic bedding. Note the presence of mud drapes in ripple cross-laminated sandstone intervals that indicate the tidal impact on sedimentation. (**D**) Storm-related coarse grained, pebbly deposits (tempestites) intecalated with mudstone. (**E**) Syneresis cracks in prodelta deposits.

4.7.2. Interpretation

FA7 is interpreted as a prodelta depositional environment. This interpretation is compatible with the stratigraphic position of this FA below delta-front deposits (FA6), at the basal parts of thickening and coarsening upward successions. The systematic repetitions of thin-bedded (1–12 cm) parallel- to ripple cross-laminated mudstone and sandstone indicate reduced depositional ratios, as well as variations in energy and sediment supply [97]. The presence of mudstone is indicative of sediment deposition under suspension during fair-weather periods, and the laminated sandstone represents deposition from river-borne currents [85]. The concurrent presence of heterolithc bedding implies that the tidal currents had an impact on the deposition of FA7. Storm currents were active during the deposition of this FA, as suggested by the presence of HCS and SCS sandstone [98]. The conglomeratic layers are interpreted as the depositional products of discrete storm episodes (tempestites) and reflect the period of storm climax [99], whereas the surrounding fine-grained sediments (mudstone) are deposited from suspension during the inter-storm periods [100]. The fining

upward trend from conglomerate into sandstone beds in some of these beds suggests decreasing in storm energy and grain-size [99].

5. Stratigraphy

The examined sedimentary rocks (approximately 1100 m thick) were described by logging and correlating five wells (Figure 1). All FA are present in all wells. The wells document the vertical facies variations that occur in the building blocks of the fluvio-deltaic system (Figure 9). The studied succession demonstrates a large-scale thickening and coarsening upward trend and evolves up sequence from mud-rich prodelta (FA7) into sand-rich delta-front (FA6) and sandy to conglomeratic delta-plain deposits (FA5, FA4, FA3 and FA2).

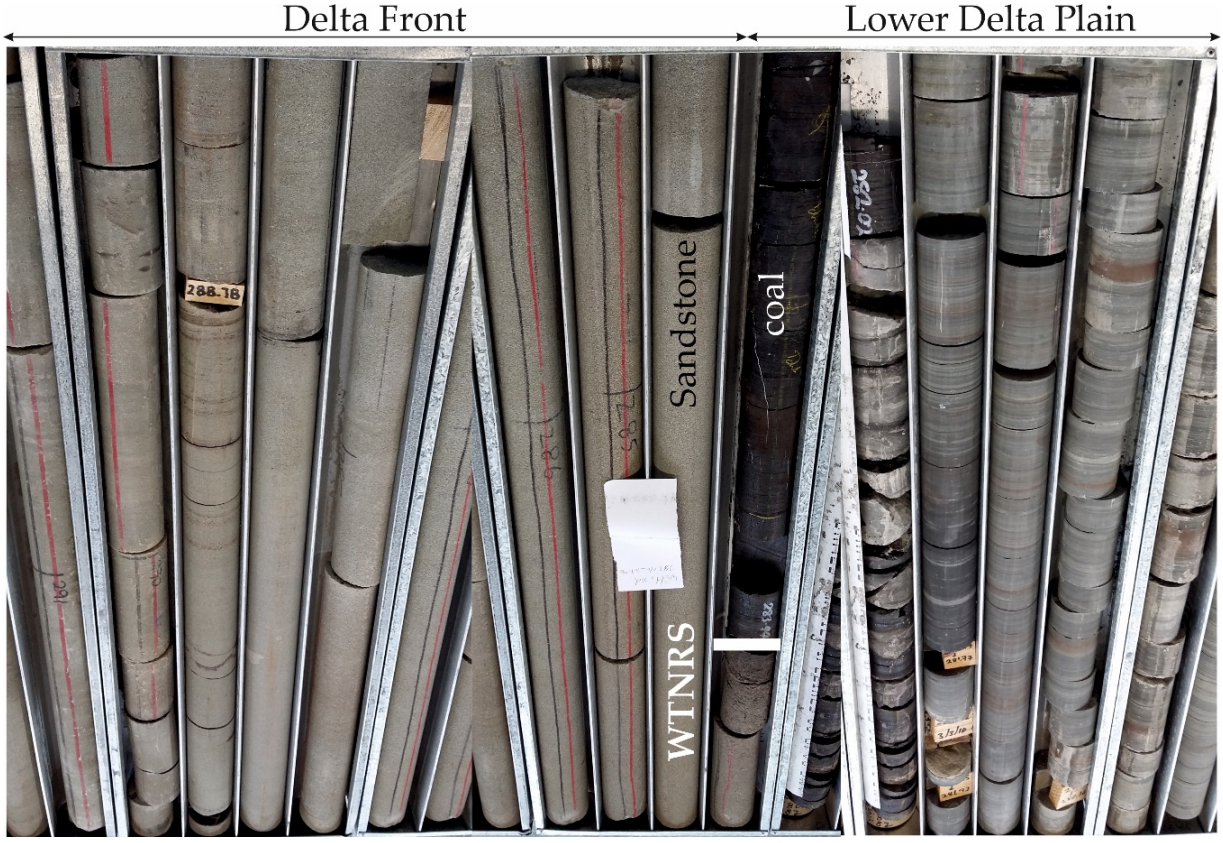


Figure 9. Core photographs illustrating the transition from delta-front to lower delta-plain deposits. Note the shift from thick-bedded, structureless sandstone (delta-front) to finer-grained heterolithics and coal-prone deposits (floodplain and overbanks of the lower delta-plain). The boundary between the two depositional environments corresponds to the within trend normal regressive surface (WTNRS) that is formed during highstand normal regression.

The delta-plain deposits are in turn overlain by conglomeratic to sandy fluvial, principally channelized deposits (FA4 and FA1). This evolution also indicates a regional shoaling upward trend for the NSB. The boundaries between the delta-front and lower delta-plain, as well as between the upper delta-plain, and fluvial deposits were recognized in all wells and correspond to sharp and/or erosional bed contacts (Figures 9 and 10).



Figure 10. Core photographs illustrating the shift from upper delta-plain to fluvial deposits. Note the abrupt increase in sediment grain-size, from fine-grained, coaly sediments (floodplains of the upper delta-plain) and tuffs to conglomeratic fluvial deposits. The boundary between the two depositional environments corresponds to the subaerial unconformity (SU), which is formed during forced regression and marks the change from highstand to lowstand normal regression.

At a smaller scale of observation, the evolution from prodelta to delta-front setting is characterized by a thickening and coarsening upward trend, with finer-grained prodelta sedimentary rocks underlying delta-front deposits. This evolution is sometimes covered by channelized sedimentary bodies that evolve into coal-prone floodplain deposits. The succession exhibits several smaller-scale transitions from prodelta to delta-front and/or coal-prone floodplain deposits that vary in thickness from 2 to 11 m (Figure 11).

They correspond to distributary mouth bars (sensu [101]) and suggest sediment source from the same terminal distributary channel. These mouth bars are stacked vertically to build thicker (up to 740 m) successions. They correspond to mouth-bar assemblages (sensu [102]), display an overall increase in the sandstone to mudstone ratio, indicating that were sourced from the same shallow downstream-bifurcating distributary channel network. The influence of volcanic activity during the deposition of the studied sedimentary rocks is documented by the tuff beds that are intercalated within the succession. Multiple tuff beds have been recognized in most FAs and occur at different stratigraphic levels, however, they are always present at the boundary between the delta-plain and the overlying fluvial deposits (Figure 10).

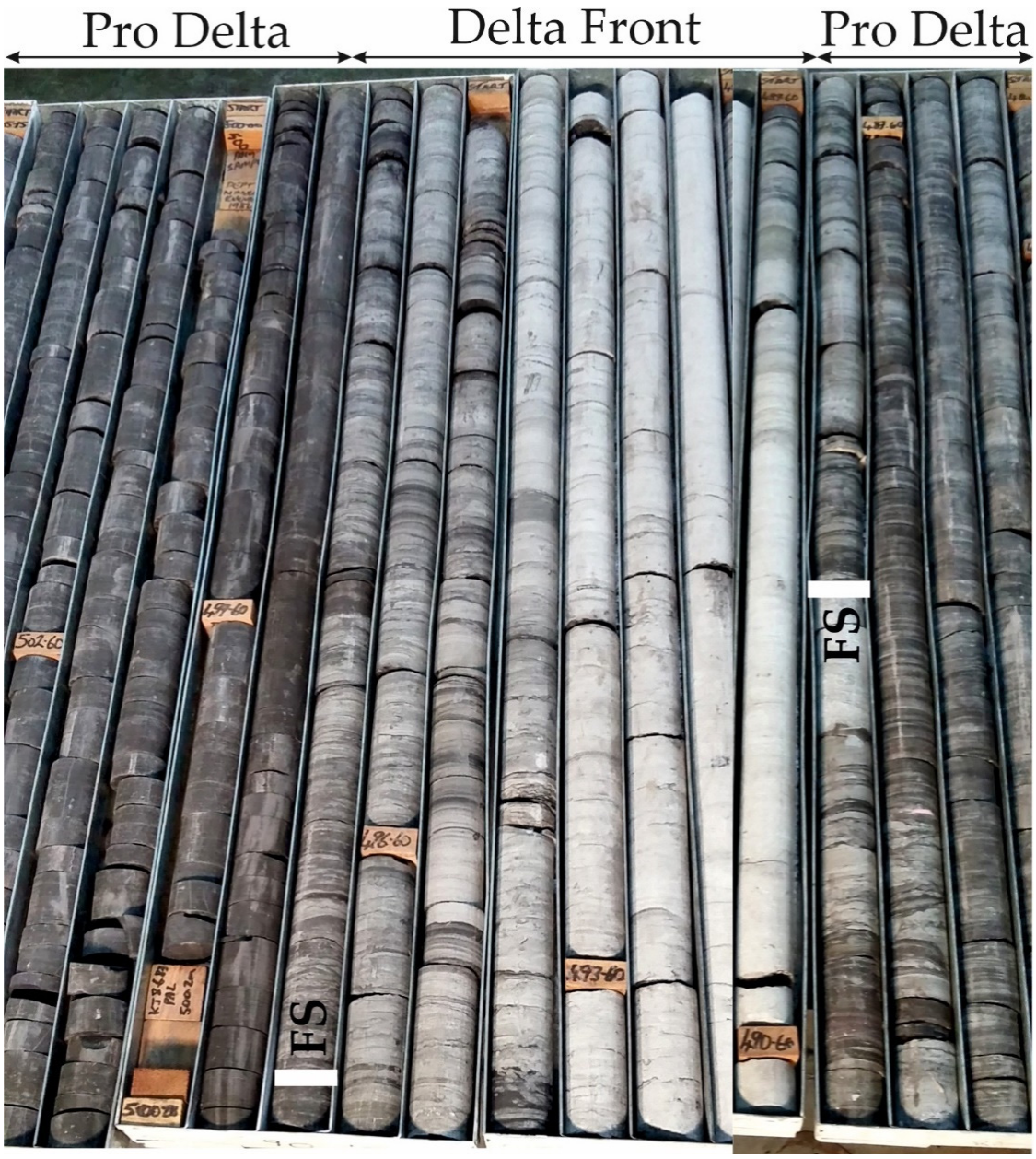


Figure 11. Core photographs illustrating the change from prodelta to delta-front deposits displaying smaller-scale coarsening and thickening upward cycles. The cycle is bounded by a surface that marks water deepening, from delta-front or delta-plain to overlying prodelta. The surface corresponds to flooding surface (FS), developed during periods of transgression.

6. Discussion

6.1. Fluvial, Tidal and Wave Contribution on Sedimentation and Palaeogeographic Implications

Outcrop-based studies on deltaic deposits have been conducted in several cases, including the Jurassic Lajas Formation [22]; the Devonian Amata and Gauja Formations [6,103] and the Upper Permian-Triassic Lambton and Moon Island sub-Groups [4,39].

The integration of sedimentological and stratigraphic data revealed that the environments and sub-environments of deposition in the study area evolve up-sequence from delta-front to lower- and upper delta-plain and fluvial deposits, indicating that the fluvio-deltaic system progrades seawards (Figure 12).

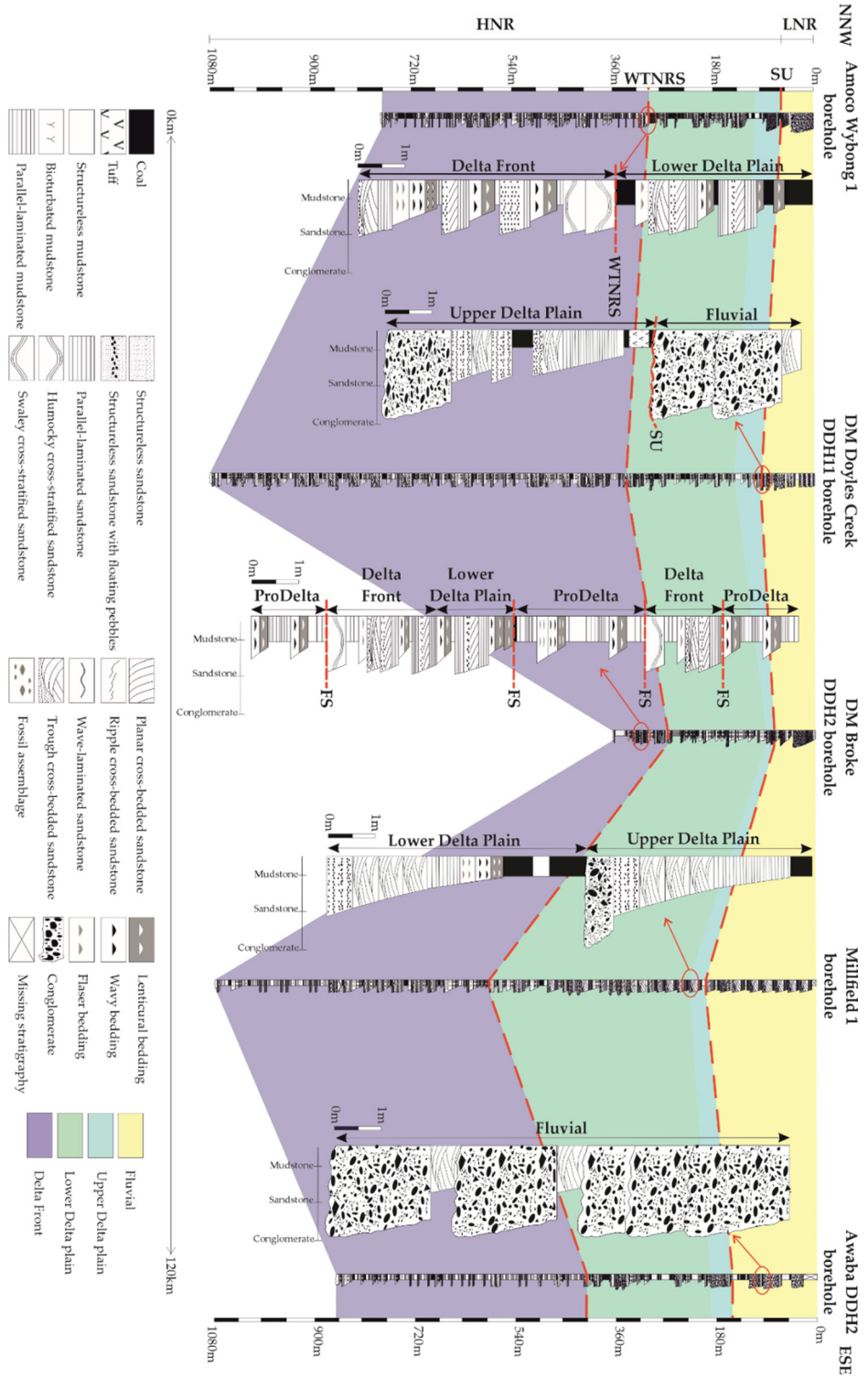


Figure 12. Correlative cross-section of the NSB illustrating the up-sequence evolution of the different depositional environments and sub-environments. The progradation of the fluvio-deltaic system and the gradual shallowing of the basin is indicated by the evolution from prodelta to delta-front, delta-plain, and finally fluvial deposits. Note that both deltaic and fluvial deposits indicate deposition during relative sea-level rise (HNR and LNR respectively), which is interrupted by relative sea-level fall (FR) at the boundary between the two systems. Abbreviations: HNR: Highstand normal regression, LNR: Lowstand normal regression, FR: Forced regression, SU: Subaerial unconformity, WRNRS: Within trend normal regression surface, FS: Flooding surface.

The influence of tides during the sediment deposition is documented by the presence of heterolithic bedding (flaser, wavy and lenticular bedding), mud drapes, and bi-directional current ripples. They occur in all depositional sub-environments of the deltaic setting (prodelta, delta-front, lower, and upper delta-plain). The intensity of the tidal influence fluctuates in the different sub-environments and thus, prodelta is significantly affected by tidal currents, in contrast to the delta-front that is only moderately affected. As such, the sedimentary structures that imply tidal influence are much more common in the prodelta, compared to delta-front. The presence of HCS/SCS and tempestites in the prodelta suggests that storm currents were also operating during the sediment deposition. In the delta-front, the waves and storm currents were the principal controlling factors whereas, tides were of secondary importance (as indicated by the prevalence of wave ripples and HCS/SCS over heterolithics). An increase in the tidal control is documented within the overlying delta-plain. However, the lower delta-plain deposits are different from the upper delta-plain deposits in terms of the abundance of the tidal in origin sedimentary structures as well as the depositional pattern and geometry of the architectural elements (Table 2).

Table 2. Comparable table that portrays the main differences between the studied Upper Permian lower and the upper delta-plain deposits.

Characteristics	Lower Delta-Plain Deposits	Upper Delta-Plain Deposits
Sediment caliber	*Lower:* (Very fine- to medium-sand).	*Higher:* (Fine- to very coarse-sand and gravel).
Sedimentary structures	*Abundance of sedimentary structures that imply tidal influence:* Mud drapes, bi-directional current ripples, flaser, wavy and lenticular bedding, spring-neap bundling of beds and thickly-stacked cross bedding. Planar cross-bedding also occurs.	*Sedimentary structures that imply tidal influence are less often but still present:* Mud drapes, and less often cross-bedding with mudstone intercalations. The main sedimentary structures include sandy and gravelly: trough cross-bedding and lamination, planar cross-bedding and lamination, parallel-stratification and lamination and clast imbrication.
Sand to mud ratio	*Lower:* The depositional sub-environment includes sandy channelized depositional units, with overbank and floodplain deposits common, forming units of substantially thickness.	*Higher:* Overbank and floodplain deposits are rare, typically with thin-beds. The depositional sub-environment includes mostly sand- to gravel-rich channelized depositional units.
Degree of amalgamation and erosion	*Lower:* The channelized units include amalgamation surfaces but usually form one-storey successions. The base of the channel-fill facies is occasionally erosional but is mostly sharp or conformable.	*Higher:* Amalgamation surfaces are abundant in the channelized units that form multi-storey successions. The base of the channel-fill facies is usually erosional but is often sharp and less commonly conformable. Scour and fill structures are often.
Dominant physical process	*Highly tidally-influenced:* The river strength is less important allowing for the redistribution of sediments through tides. The wave action is of secondary importance.	*Fluvial-dominated:* The river currents are the principal processes that control the sediment deposition. The tides are less important and slightly modulate the succession. The wave action is of secondary importance.

In the lower delta-plain, the impact of tides is widespread and the proportion of sedimentary units with mudstone drapes and heterolithic bedding is very common. In the upper delta-plain, fluvial action is the dominant physical process that governs the sediment deposition. Fluvial sediments dominate and mud drapes (and less often cross-bedding with mudstone intercalations) are structures that independently imply active tidal currents during the deposition. Further, the lower delta-plain facies are typified by lower sediment caliber, sand to mud ratio and, degree of amalgamation and erosion, compared to the upper delta-plain facies. The impact of waves in the studied delta-plain deposits is not great.

The overlying fluvial deposits exhibit no evidence of tidal currents and the deposition is controlled by fluvial currents.

Similar upward increase in the degree of tidal impact on sedimentation across the boundary between the delta-front and delta-plain deposits has been described in outcrops in different parts of the NSB [4]. This trend has been interpreted as the result of regional constraints that are associated to tectonic activity and confinement. Additional explanation for this reduced tidal signature in the delta-front deposits is the steep character of the delta-front that reduces development and preservation potential of the tidal signatures [46]. The common presence of tidally-related sedimentary structures in the delta-plain deposits suggests that the fluvial currents were not of sufficient strength to preclude the influence of tidal reworking. The decrease in their abundance across the delta-plain (from lower to upper delta-plain) is indicative of fluvio-deltaic progradation and gradual prevalence of continental (fluvial) over basinal (tides) parameters. In the Jurassic Lajas Formation (Argentina), the increased topographic slopes have been invoked to account for the fluvio-deltaic progradation [11,22]. Sedimentary structures that imply wave action exist in the studied succession, especially in the prodelta deposits, but are generally rare in the other depositional sub-environments. The supremacy of fluvial and tidal currents over wave currents in the sediment deposition has been, for instance, identified in the Middle Devonian Gauja Formation, Baltic Basin [6], as well as in other parts of the NSB [4]. In both cases, the restricted influence of waves on sedimentation has been explained with gradual acceleration of the fluvial contribution (progradation) and with powerful tidal action that minimized the preservation of wave-related sedimentary structures. The observed sudden shift in the dominant sedimentary processes, from basinal (tides and/or waves) to continental (fluvial) across the boundary between the upper delta-plain and fluvial deposits could be related to regional tectonics and basin confinement. This combination could be responsible for the augmented fluvial energy and associated input of coarse-grained material in the NSB. Such interpretation agrees with the regional geological framework that suggests uplift and erosion of the New England Orogen during the Hunter–Bowen Orogeny [104]. Limited or no impact of tidal currents on the fluvial deposits have been described in other parts of the NSB and in the Lajas Formation, Argentina (Jurassic). In both cases, this observation has been associated with steep topography [4,16].

6.2. Sequence Stratigraphic Implications

Sequence stratigraphy enables conclusions regarding the depositional response in sedimentary basins to both external (e.g., tectonics, eustatic changes and climate) and internal (e.g., delta-switching and shoreline autoretreat) parameters (e.g., [68,69,105–109]). The reconstruction of the sequence stratigraphic framework is based on the recognition of stratal stacking patterns, which in turn define shoreline trajectories and the development of the systems tracts [110].

The up-sequence development of the depositional environments and sub-environments in the NSB indicates progradation and aggradation of the deltaic system and subsequent erosion by fluvial action. These features conform to a forestepping and upstepping shoreline trajectory, which defines normal regression (Figure 12). The succession is typified by smaller-scale coarsening and thickening upward cycles at the lower stratigraphic levels that are represented by prodelta and delta-front deposits, capped often by delta-plain and floodplain/overbank deposits (Figure 12). These cycles are interpreted as higher frequency cycles, which were developed in response to small-amplitude, short-term fluctuations in the relative contribution of sedimentation and accommodation. They form when the rates of creation of accommodation are lower than the sedimentation rates, resulting in basinward shoreline migration [107,110]. The delta-plain deposits at the top of each high-frequency sequence sometimes exhibit erosional contacts with the underlying delta-front, but the lower boundary is relatively planar over the study area (Figure 12). This suggests deposition during normal regression [106,111]. Each high-frequency sequence is bounded by a lithological discontinuity that marks abrupt water deepening, from delta-front or

delta-plain to overlying prodelta (Figure 10). Such surfaces correspond to flooding surfaces (FS, sensu [46]), developed during periods of transgression (T), which end the coarsening upward trend of each deltaic sedimentation cycle. However, flooding surfaces are allostratigraphic contacts, and their precise sequence stratigraphic meaning needs to be assessed on a case by case basis [112].

Up-sequence, the boundary between the delta-front and the coal-bearing delta-plain deposits is represented by a surface, which is either erosional or planar (Figure 12). In some cases, this surface is related to lithological contrast (sandy delta-front underlays muddied, coaly floodplain deposits of the delta-plain) whereas in others, it develops within similar lithologies (sandy delta-front deposits underlay sandy delta-plain channelized deposits). These observations, in conjunction with the shallowing upward trend across this surface suggest progradation and aggradation during the deposition of the sedimentary rocks. This surface is interpreted as a within-trend normal regressive surface and indicates normal regression of the shoreline (WTNRS, sensu [113]). Further up-sequence, the succession displays a sudden increase in the sediment caliber (from mostly sandy-conglomeratic delta-plain to conglomeratic fluvial deposits) and power of the dominant currents across the boundary between the delta-plain and the fluvial deposits. These features, in conjunction with the erosional character of the fluvial over the deltaic deposits suggest that the underlying deltaic sedimentary rocks were deposited during the highstand systems tract (HST) and the overlying fluvial deposits during the lowstand systems tract (LST, Figure 12). Their boundary is interpreted as the subaerial unconformity (SU) that was developed during the falling-stage systems tracts (FSST). Both depositional environments were formed during periods of relative sea-level rise, when sedimentation rates exceeded the rates of this rising. In contrast, the SU signifies a period of relative sea-level fall, possibly enhanced by tectonic activity.

In summary, the proposed sequence stratigraphic framework for the studied deposits suggests deltaic deposition during HNR and the overlying fluvial setting during LNR. In this scenario, the delta-front and the associated higher frequency cycles were developed during HNR that was interrupted by small periods of transgression and formation of FS's. Comparable sequence stratigraphic framework has been proposed from outcrop data in other parts of the NSB [4]. In both cases, this framework requires a constant increase in the sediment input through the sediment routing systems into the NSB, indicating active tectonics during the sedimentation and agrees with the regional geology. The structural regime is governed by the Peel-Manning Fault System (within the New England Orogen) that is characterized by Middle to Late Permian folding and Late Permian–Early Triassic dispersal of tectonostratigraphic blocks [104]. This activity caused uplift of the New England Orogen whereas, the associated erosion prompted transport of coarse-grained material and deposition in the NSB (the Permo-Triassic megacycle of Conaghan [114]).

7. Conclusions

Detailed sedimentological investigation of the Upper Permian sedimentary succession (Wittingham, Tomago and Newcastle Coal Measures) provides useful new data and insights into the geological evolution of the Northern Sydney Basin, southeast Australia. The principal concluding remarks are related to the: (1) documentation of environments and sub-environments of deposition and their stratigraphic evolution, (2) relative contribution of the main depositional processes and, (3) paleogeographic implications.

- The studied sedimentary rocks are composed of fifteen facies and are grouped into seven facies associations that correspond to deltaic (prodelta, delta-front, lower and upper delta-plain) and fluvial depositional environments.
- These Lower Permian sedimentary rocks reflect the variable temporal balance in the impact of storm/wave and tidal processes. The deltaic system records the prevalence of tidal currents during the deposition, with abundance of tidal sedimentary structures.
- A tidally-influenced, regressive fluvio-deltaic depositional setting is envisaged based on the: (1) Stratigraphic evolution that illustrates a large-scale shoaling upward trend, from prodelta deposits, through delta-front and delta-plain sedimentary rocks to

fluvial environments of deposition, (2) General coarsening upward trend that implies progradation, and (3) Lack of deepening upward successions.

- This deltaic system illustrates an up-section deceleration in the tidal influence, with an associated increase in the fluvial energy. As such, sedimentary structures of tidal origin are abundant in the prodelta and lower delta-plain deposits, become less frequent in the upper delta-plain sediments, and eventually become almost absent in the overlying fluvial system.
- This system occurs along the entire studied region, which is volcanically active. Tuff beds are common in the succession and occur at several stratigraphic levels. However, the fluvio-deltaic boundary is characterized by intense volcanism that is recorded throughout the study area.

Author Contributions: Conceptualization, A.G.M., O.C. and W.J.C.; Data curation, S.M., C.B. and A.G.M.; Formal analysis, S.M.; Project administration, K.R. and E.H.; Resources, K.R. and E.H.; Software, C.B.; Supervision, A.G.M. and W.J.C.; Writing—original draft, S.M.; Writing—review & editing, A.G.M. and O.C. All authors have read and agreed to the published version of the manuscript.

Funding: This research was sponsored by the Geological Survey of New South Wales (GSNSW), through the research project "Unravelling long-distance stratigraphic correlations of the Northern Sydney Basin".

Institutional Review Board Statement: Not applicable.

Informed Consent Statement: Not applicable.

Acknowledgments: This research was sponsored by the Geological Survey of New South Wales (GSNSW), through the research project "Unravelling long-distance stratigraphic correlations of the Northern Sydney Basin". The authors acknowledge the journal editor Luca Mao and the three anonymous reviewers for their valuable comments that greatly improved the manuscript. Authors wish to acknowledge Bill Landenberger for constructive and valuable discussions about the basin-fill conditions in the northern Sydney Basin. Our colleague Jake Breckenridge is thanked for his patient conversation and insights during this study. Mark Ryland (GSNSW) is also thanked for his hard work and physical labor in setting up cores for inspection at the Londonderry Drillcore Library.

Conflicts of Interest: The authors declare no conflict of interest.

References

1. Martinius, A.W.; Kaas, I.; Naess, A.; Helgesen, G.; Kjaerefjord, J.M.; Keith, D.A. Sedimentology of heterolithic and tide-dominated Tilje Formation (Early Jurassic, Halten Terrace, offshore mid-Norway). In *Sedimentary Environments Offshore Norway-Paleozoic to Recent: Norwegian Petroleum Foundation Special Publication*; Martinsen, O.J., Dreyer, T., Eds.; Elsevier: Amsterdam, The Netherlands, 2001; Volume 10, pp. 103–144.
2. Legler, B.; Johnson, H.D.; Hampson, G.J.; Massart, B.Y.G.; Jackson, C.A.L.; Jackson, M.D.; El-Barkooky, A.; Ravnas, R. Facies model of a fine-grained, tide-dominated delta: Lower Dir Abu Lifa Member (Eocene), Western Desert, Egypt. *Sedimentology* **2013**, *60*, 1313–1356. [CrossRef]
3. Boyd, R.; Dalrymple, R.W.; Zaitlin, B.A. Estuarine and Incised-Valley Facies Models. *Facies Models Revisit.* **2006**, *84*, 171–235.
4. Breckenridge, J.; Maravelis, A.G.; Catuneanu, O.; Ruming, K.; Holmes, E.; Collins, W.J. Outcrop analysis and facies model of an Upper Permian tidally influenced fluvio-deltaic system: Northern Sydney Basin, SE Australia. *Geol. Mag.* **2019**, *156*, 1715–1741. [CrossRef]
5. Willis, B.J.; Gabel, S.L. Sharp-based, tide-dominated deltas of the Sego sandstone, Book Cliffs, Utah, USA. *Sedimentology* **2001**, *46*, 479–506. [CrossRef]
6. Pontén, A.; Plink-Björklund, P. Depositional environments in an extensive tide-influenced delta plain, Middle Devonian Gauja Formation, Devonian Baltic Basin. *Sedimentology* **2007**, *54*, 969–1006. [CrossRef]
7. Pontén, A.; Plink-Björklund, P. Regressive to transgressive transits reflected in tidal bars, Middle Devonian Baltic Basin. *Sediment. Geol.* **2009**, *218*, 48–60. [CrossRef]
8. Porebski, S.J.; Steel, R.J. Deltas and sea-level change. *J. Sediment. Res.* **2006**, *76*, 390–403. [CrossRef]
9. Ainsworth, R.B.; Vakarelov, B.K.; Nanson, R.A. Dynamic spatial and temporal prediction of changes in depositional processes on clastic shorelines: Toward improved subsurface uncertainty reduction and management. *AAPG Bull.* **2011**, *95*, 267–297. [CrossRef]
10. Plink-Björklund, P. Effects of tides on deltaic deposition: Causes and responses. *Sediment. Geol.* **2012**, *279*, 107–133. [CrossRef]

11. Rossi, V.M.; Steel, R.J. The role of tidal, wave and river currents in the evolution of mixed-energy deltas: Example from the Lajas Formation (Argentina). *Sedimentology* **2016**, *63*, 824–864. [CrossRef]
12. Dalrymple, R.W.; Zaitlin, B.A.; Boyd, R. Estuarine facies models: Conceptual basis and stratigraphic implications. *J. Sediment. Petrol.* **1992**, *62*, 1130–1146. [CrossRef]
13. Plink-Björklund, P. Stacked fluvial and tide-dominated estuarine deposits in high-frequency (fourth-order) sequences of the Eocene Central Basin, Spitsbergen. *Sedimentology* **2005**, *52*, 391–428. [CrossRef]
14. Dalrymple, R.W.; Choi, K. Morphologic and facies trends through the fluvial–marine transition in tide-dominated depositional systems: A schematic framework for environmental and sequence-stratigraphic interpretation. *Earth Sci. Rev.* **2007**, *81*, 135–174. [CrossRef]
15. Stewart, R.; Adler, D. *New South Wales Petroleum Potential. Coal and Petroleum Geology Branch Bulletin 1, 5–36*; New South Wales Department of Mineral Resources: Sydney, Australia, 1995.
16. Alder, J.; Hawley, S.; Maung, T.; Scott, J.; Shaw, R.; Sinelnikov, A.; Kouzmina, G. Prospectivity of the Offshore Sydney Basin: A New Perspective. *APPEA J.* **1998**, *38*, 68–92. [CrossRef]
17. Montoya, D. *Coal Seam Gas Royalties in Australian States & Territories*; NSW Parliament: Sydney, Australia, 2012.
18. Maravelis, A.; Chamilaki, E.; Pasadakis, N.; Zelilidis, A.; Collins, W.J. Hydrocarbon generation potential of a Lower Permian sedimentary succession (Mount Agony Formation): Southern Sydney Basin, New South Wales, Southeast Australia. *Int. J. Coal Geol.* **2017**, *183*, 52–64. [CrossRef]
19. Maravelis, A.; Chamilaki, E.; Pasadakis, N.; Vassiliou, A.; Zelilidis, A. Organic geochemical characteristics and paleodepositional conditions of an Upper Carboniferous mud-rich succession (Yagon Siltstone): Myall Trough, southeast Australia. *J. Pet. Sci. Eng.* **2017**, *158*, 322–335. [CrossRef]
20. Palozzi, J.; Pantopoulos, G.; Maravelis, A.G.; Nordsvan, A.; Zelilidis, A. Sedimentological analysis and bed thickness statistics from a Carboniferous deep-water channel-levee complex: Myall Trough, SE Australia. *Sediment. Geol.* **2018**, *364*, 160–179. [CrossRef]
21. Holz, M.; Kalkreuth, W.; Banerjee, I. Sequence stratigraphy of paralic coal-bearing strata: An overview. *Int. J. Coal Geol.* **2002**, *48*, 147–179. [CrossRef]
22. McIlroy, D.; Flint, S.S.; Howell, J.A.; Timms, N. Sedimentology of the tide-dominated Jurassic Lajas Formation, Neuqu en Basin, Argentina. *Geol. Soc. Lond. Spec. Publ.* **2005**, *252*, 83–107. [CrossRef]
23. Desjardins, P.R.; Buatois, L.A.; Pratt, B.R.; Mangano, G. Forced regressive tidal flats: Response to falling sea level in tide-dominated settings. *J. Sediment. Res.* **2012**, *82*, 149–162. [CrossRef]
24. Chen, S.; Steel, R.J.; Dixon, J.F.; Osman, A. Facies and architecture of a tide-dominated segment of the Late Pliocene Orinoco Delta (Morne L'Enfer Formation) SW Trinidad. *Mar. Pet. Geol.* **2014**, *57*, 208–232. [CrossRef]
25. Lv, D.; Chen, J. Depositional environments and sequence stratigraphy of the Late Carboniferous À Early Permian coal-bearing successions (Shandong Province, China): Sequence development in an epicontinental basin. *J. Asian Earth Sci.* **2014**, *79*, 16–30. [CrossRef]
26. Zelilidis, A.; Kontopoulos, N. Plio-Pleistocene alluvial architecture in marginal extensional narrow sub-basins: Examples from southwest Greece. *Geol. Mag.* **1999**, *136*, 241–262. [CrossRef]
27. Lan, C.; Yang, M.; Zhang, Y. Impact of sequence stratigraphy, depositional facies and diagenesis on reservoir quality: A case study on the Pennsylvanian Taiyuan sandstones, northeastern Ordos Basin, China. *Mar. Pet. Geol.* **2016**, *69*, 216–230. [CrossRef]
28. Warbrooke, P.R. Depositional Environments of the Upper Tomago and Lower Newcastle Coal Measures, New South Wales. Ph.D. Thesis, University of Newcastle, Callaghan, Australia, 1981.
29. Diessel, C.F.K. *Coal-Bearing Depositional Systems*; Springer: Berlin/Heidelberg, Germany, 1992; p. 721.
30. Agnew, D.; Bocking, M.; Brown, K.; Ives, M.; Johnson, D.; Howes, M.; Preston, B.; Rigby, R.; Warbrooke, P.; Weber, C.R. Sydney Basin—Newcastle Coalfield. In *Geology of Australian Coal Basins*; Ward, C.R., Harrington, H.J., Mallett, C.W., Beeston, J.W., Eds.; Coal Geology Group, Special Publication; Geological Society of Australia Inc.: Hornsby, Australia, 1995; Volume 1, pp. 197–212.
31. Herbert, C. Sequence stratigraphy of the Late Permian Coal Measures in the Sydney Basin. *Aust. J. Earth Sci.* **1995**, *42*, 391–405. [CrossRef]
32. Herbert, C. Relative sea level control of deposition in the Late Permian Newcastle Coal Measures of the Sydney Basin, Australia. *Sediment. Geol.* **1997**, *107*, 167–187. [CrossRef]
33. Stevenson, D. *Broke Drilling Programme Geological Report*; Geological Survey Report No. GS 1999/277; Department of Mineral Resources: St. Leonards, Australia, 1999.
34. Creech, M.K.; Ives, M.; Stevenson, D.; Brunton, J.; Rigby, R.; Leary, S.; Graham, P.; Smith, C.; Atkins, B.; Knight, C.; et al. A revision of the stratigraphy of the Wollombi Coal Measures. *Minfo* **2004**, *81*, 24–25.
35. Fielding, C.R.; Frank, T.D.; Tevyaw, A.P.; Savatic, K.; Vajda, V.; McLoughlin, S.; Crowley, J.L. Sedimentology of the continental end-Permian extinction event in the Sydney Basin, eastern Australia. *Sedimentology* **2021**, *68*, 30–62. [CrossRef]
36. Fielding, C.R.; Frank, T.D.; McLoughlin, S.; Vajda, V.; Mays, C.; Tevyaw, A.P.; Winguth, A.; Winguth, C.; Nicoll, R.S.; Bocking, M.; et al. Age and pattern of southern high-latitude continental end-Permian extinction constrained by multiproxy analysis. *Nat. Commun.* **2019**, *10*, 385. [CrossRef]

37. McLoughlin, S.; Nicoll, R.S.; Crowley, J.L.; Vajda, V.; Mays, C.; Fielding, C.R.; Frank, T.D.; Wheeler, A.; Bocking, M. Age and Paleoenvironmental Significance of the Frazer Beach Member—A New Lithostratigraphic Unit Overlying the End-Permian Extinction Horizon in the Sydney Basin, Australia. *Front. Earth Sci.* **2021**, *8*, 600976. [CrossRef]
38. Metcalfe, I.; Crowley, J.L.; Nicoll, R.S.; Schmitz, M. High-precision U-Pb CA-TIMS calibration of Middle Permian to Lower Triassic sequences, mass extinction and extreme climate-change in eastern Australian Gondwana. *Gondwana Res.* **2015**, *28*, 61–81. [CrossRef]
39. Maravelis, A.G.; Breckenridge, J.; Ruming, K.; Holmes, E.; Amelin, Y.; Collins, W.J. Re-assessing the Upper Permian Stratigraphic Succession of the Northern Sydney Basin, Australia, by CA-IDTIMS. *Geosciences* **2020**, *10*, 474. [CrossRef]
40. Hawley, S.P.; Glen, R.A.; Baker, C.J. *Newcastle Coalfield Regional Geology Sheet 1:100 000*; New South Wales Department of Mineral Resources: Sydney, Australia, 1995.
41. Percival, I.G.; Meakin, N.S.; Sherwin, L.; Vanderlaan, T.A.; Flitcroft, P.A. Permian fossils and palaeoenvironments of the northern Sydney Basin, New South Wales. *Q. Notes* **2012**, *138*, 1–22.
42. Crawford, T.J.; Meffre, S.; Squire, R.J.; Barron, L.M.; Falloon, T.J. Middle and Late Ordovician magmatic evolution of the Macquarie Arc, Lachlan Orogen, New South Wales. *Aust. J. Earth Sci.* **2007**, *54*, 181–214. [CrossRef]
43. Scheibner, E. *Explanatory Notes on the Tectonic Map of New South Wales, Scale 1:1,000,000*; New South Wales Geological Survey: Sydney, Australia, 1976; p. 283.
44. Jones, J.G.; Conaghan, P.J.; McDonnell, K.L.; Flood, P.H.; Royce, K. Papuan analogue and a foreland basin model for the Bowen–Sydney Basin. In *The Phanerozoic Earth History of Australia*; Veevers, J.J., Ed.; Oxford University Press: Oxford, UK, 1984; pp. 243–261.
45. Danis, C.; Daczko, N.R.; Lackie, M.; Craven, S.J. Retrograde metamorphism of the Wongwibinda Complex, New England Fold Belt and the implications of 2.5D subsurface geophysical structure for the metamorphic history. *Aust. J. Earth Sci.* **2010**, *57*, 357–375. [CrossRef]
46. Collins, W.J. A reassessment of the 'Hunter-Bowen Orogeny': Tectonic implications for the southern New England fold belt. *Aust. J. Earth Sci.* **1991**, *38*, 409–423. [CrossRef]
47. Landenberger, B.; Farrell, T.; Offler, R.; Collins, W.; Whitford, D. Tectonic implications of Rb_Sr biotite ages for the Hillgrove Plutonic Suite, New England Fold Belt, NSW, Australia. *Precambrian Res.* **1995**, *71*, 251–263. [CrossRef]
48. Belica, M.; Tohver, E.; Pisarevsky, S.; Jourdan, F.; Denyszyn, S.W.; George, A.D. Middle Permian paleomagnetism of the Sydney Basin, Eastern Gondwana: Testing Pangea models and the timing of the end of the Kiaman Reverse Superchron. *Tectonophysics* **2017**, *699*, 178–198. [CrossRef]
49. Jenkins, R.B.; Offler, R. Metamorphism and deformation of an Early Permian extensional basin sequence: The Manning Group, southern New England Orogen. *Aust. J. Earth Sci.* **1996**, *43*, 423–435. [CrossRef]
50. Williams, M.; Jones, B.G.; Carr, P. Geochemical consequences of the Permian–Triassic mass extinction in a non-marine succession, Sydney Basin, Australia. *Chem. Geol.* **2012**, *326*, 174–188. [CrossRef]
51. Veevers, J.J.; Conaghan, P.J.; Powell, C.M. *Eastern Australia, Permian–Triassic Pangean Basins and Foldbelts along the Panthalassan Margin of Gondwanaland*; Geological Society of America: Boulder, CO, USA, 1994; Volume 174, pp. 11–171.
52. Korsch, R.; Totterdell, J.M.; Cathro, D.L.; Nicoll, M.G. Early Permian East Australian Rift System. *Aust. J. Earth Sci.* **2009**, *56*, 381–400. [CrossRef]
53. Li, P.; Rosenbaum, G.; Vasconcelos, P. Chronological constraints on the Permian geodynamic evolution of eastern Australia. *Tectonophysics* **2014**, *617*, 20–30. [CrossRef]
54. Roberts, J.L.; Offler, R.; Fanning, M.; Fanning, C. Carboniferous to Lower Permian stratigraphy of the southern Tamworth Belt, southern New England Orogen, Australia: Boundary sequences of the Werrie and Rouchel blocks. *Aust. J. Earth Sci.* **2006**, *53*, 249–284. [CrossRef]
55. Armstrong, M.; Bamberry, W.J.; Hutton, A.; Jones, B.G. Sydney Basin—Southern Coalfield 1995. In *Geology of Australian Coal Basins*; Ward, C.R., Harrington, H.J., Mallett, C.W., Beeston, J.W., Eds.; Geological Society of Australia Coal Geology Group: Sydney, Australia, 1995; Volume 1, pp. 213–230.
56. Bamberry, W.J.; Hutton, A.C.; Jones, B.G. The Permian Illawarra Coal Measures, southern Sydney Basin, Australia: A case study of deltaic sedimentation. In *Geology of Deltas*; Oti, M., Postma, G., Eds.; Balkema: Rotterdam, The Netherlands, 1995; pp. 153–167.
57. Veevers, J. Updated Gondwana (Permian–Cretaceous) earth history of Australia. *Gondwana Res.* **2006**, *9*, 231–260. [CrossRef]
58. Jenkins, R.B.; Landenberger, B.; Collins, W.J. Late Palaeozoic retreating and advancing subduction boundary in the New England Fold Belt, New South Wales. *Aust. J. Earth Sci.* **2002**, *49*, 467–489. [CrossRef]
59. McNally, G.H.; Branagan, D.F. Geotechnical consequences of the Newcastle Coal Measures rocks. *Aust. J. Earth Sci.* **2013**, *61*, 363–374. [CrossRef]
60. Mantle, D.J.; Kelman, A.P.; Nicoll, R.S.; Laurie, J.R. *Australian Biozonation Chart*; Geoscience Australia: Canberra, Australia, 2010. Available online: http://www.ga.gov.au/metadata-gateway/metadata/record/gcat_70371 (accessed on 22 November 2020).
61. Dehghani, M.H. Sedimentology, Genetic Stratigraphy and Depositional Environment of the Permo-Triassic Succession in the Southern Sydney Basin, Australia. Ph.D. Thesis, University of Wollongong, Wollongong, Australia, 1994.
62. Retallack, G.J. Postapocalyptic greenhouse paleoclimate revealed by earliest Triassic paleosols in the Sydney Basin, Australia. *Geol. Soc. Am. Bull.* **1999**, *111*, 52–70. [CrossRef]

63. White, R.V.; Saunders, A. Volcanism, impact and mass extinctions: Incredible or credible coincidences? *Lithos* **2005**, *79*, 299–316. [CrossRef]
64. Holcombe, R.; Stephens, C.; Fielding, C.; Gust, D.; Little, T.; Sliwa, R.; Kassan, J.; McPhie, J.; Ewart, A. Tectonic evolution of the northern New England Fold Belt: The Permian–Triassic Hunter–Bowen event. *Tecton. Metallog. N. Engl. Orogen* **1997**, *19*, 52–65.
65. Li, P.F.; Rosenbaum, G.; Rubatto, D. Triassic asymmetric subduction rollback in the southern New England Orogen (eastern Australia): The end of the Hunter-Bowen Orogeny. *Aust. J. Earth Sci.* **2012**, *59*, 965–981. [CrossRef]
66. Nichols, G.J.; Fisher, J.A. Processes, facies and architecture of fluvial distributary system deposits. *Sediment. Geol.* **2007**, *195*, 75–90. [CrossRef]
67. Catuneanu, O.; Khalifa, M.A.; Wanas, H.A. Sequence stratigraphy of the Lower Cenomanian Bahariya Formation, Bahariya Oasis, Western Desert, Egypt. *Sediment. Geol.* **2016**, *190*, 121–137. [CrossRef]
68. Di Celma, C.; Cantalamessa, G.; Landini, W.; Ragaini, L. Stratigraphic evolution from shoreface to shelf-indenting channel depositional systems during transgression: Insights from the lower Pliocene Súa Member of the basal Upper Onzole Formation, Borbon Basin, northwest Ecuador. *Sediment. Geol.* **2010**, *223*, 162–179. [CrossRef]
69. Maravelis, A.G.; Boutelier, D.; Catuneanu, O.; Seymour, K.S.; Zelilidis, A. A review of tectonics and sedimentation in a forearc setting: Hellenic Thrace Basin, north Aegean Sea and northern Greece. *Tectonophysics* **2016**, *674*, 1–19. [CrossRef]
70. Lloret, J.; Ronchi, A.; López-Gómez, J.; Arche, A.; De la Horra, R.; Barrenechea, J.; Gretter, N. Syn-tectonic sedimentary evolution of the continental late Palaeozoic-early Mesozoic Erill Castell-Estac Basin and its significance in the development of the central Pyrenees Basin. *Sediment. Geol.* **2018**, *374*, 134–157. [CrossRef]
71. Miall, A.D. *The Geology of Fluvial Deposits: Sedimentary Facies, Basin Analysis, and Petroleum Geology*; Springer: Berlin/Heidelberg, Germany, 1996.
72. Nemec, W.; Postma, G. Quaternary alluvial fans in southwestern Crete: Sedimentation processes and geomorphic evolution. Alluvial Sedimentation—Special Publications. *Int. J. Sedimentol.* **1993**, *17*, 235–276.
73. Nemec, W.; Steel, R.J. Alluvial and coastal conglomerates: Their significant features and some comments on gravelly mass-flow deposits. *Sedimentol. Gravels Conglom.* **1984**, *10*, 1–31.
74. Collinson, J.D. *Alluvial Sediments*; Blackwell Science: Hoboken, NJ, USA, 1996.
75. Collinson, J.D.; Mountney, N.P.; Thompson, D. *Sedimentary Structures*, 3rd ed.; Terra Publishing: Harpenden, UK, 2006.
76. Moretti, M.; Ronchi, A. Liquefaction features interpreted as seismites in the Pleistocene fluvio-lacustrine deposits of the Neuquén Basin (Northern Patagonia). *Sediment. Geol.* **2011**, *235*, 200–209. [CrossRef]
77. Bridge, J.S. *Fluvial Facies Models: Recent Developments*; Facies Models Revisited; Special Publication; SEPM: Tulsa, OK, USA, 2006; Volume 84, pp. 85–170.
78. Allen, J.R.L. Sedimentary Processes and Facies in the Gironde Estuary: A Recent Model for Macrotidal Estuarine Systems. *Can. Soc. Pet. Geol. Spec. Publ.* **1991**, *16*, 29–39.
79. Allen, J.R.L. Sand waves: A model of origin and internal structure. *Sediment. Geol.* **1980**, *26*, 281–328. [CrossRef]
80. Marchetti, L.; Ronchi, A.; Santi, G.; Voigt, S. The Gerola Valley site (Orobic Basin, Northern Italy): A key for the understanding of late Early Permian tetrapod ichnofaunas. *Palaeogeogr. Palaeoclimatol. Palaeoecol.* **2015**, *439*, 95–116. [CrossRef]
81. Berra, F.; Felletti, F. Syndepositional tectonics recorded by soft-sediment deformation and liquefaction structures (continental Lower Permian sediments, Southern Alps, Northern Italy): Stratigraphic significance. *Sediment. Geol.* **2011**, *235*, 249–263. [CrossRef]
82. Mellere, D.; Steel, R.J. Tidal Sedimentation in Inner Hebrides Half Grabens, Scotland: The Mid-Jurassic Bearreraig Sandstone Formation. *Geol. Soc. Lond. Spec. Publ.* **1996**, *117*, 49–79. [CrossRef]
83. Visser, M.J. Neap-Spring cycles reflected in Holocene subtidal large-scale bedform deposits: A preliminary note. *Geology* **1980**, *8*, 543–546. [CrossRef]
84. Nio, S.D.; Yang, C.S. Sea-level fluctuations and geometric variability of tide-dominated sandbodies. *Sediment. Geol.* **1991**, *70*, 161–193. [CrossRef]
85. Hampton, B.A.; Horton, B.K. Sheetflow fluvial processes in a rapidly subsiding basin, Altiplano plateau, Bolivia. *Sedimentology* **2007**, *54*, 1121–1148. [CrossRef]
86. Buatois, L.A.; Santiago, N.; Herrera, M.; Plink-Björklund, P.; Steel, S.; Espin, M.; Parra, K. Sedimentological and ichnological signatures of changes in wave, river and tidal influence along a Neogene tropical deltaic shoreline. *Sedimentology* **2012**, *59*, 1568–1612. [CrossRef]
87. Guion, P.D.; Fulton, I.M.; Jones, N.S. Sedimentary facies of the coalbearing Westphalian A and B north of the Wales-Brabant High. In *European Coal Geology*; Whateley, M.K.G., Spears, D.A., Eds.; Special Publication No. 82; Geological Society of London: London, UK, 1995; pp. 45–78.
88. Davies, R.; Howell, J.; Boyd, R.; Flint, S.; Diessel, C. High-resolution sequence stratigraphic correlation between shallow-marine and terrestrial strata: Examples from the Sunnyside Member of the Cretaceous Blackhawk Formation, Book Cliffs, eastern Utah. *Am. Assoc. Pet. Geol.* **2006**, *90*, 1121–1140. [CrossRef]
89. Myrow, P.M.; Southard, J.B. Combined-flow model for vertical stratification sequences in shallow marine storm-deposited beds. *J. Sediment. Petrol.* **1991**, *61*, 202–210.
90. Ghani, M.; Bhattacharya, J.P. Basic Building Blocks and Process Variability of a Cretaceous Delta: Internal Facies Architecture Reveals a More Dynamic Interaction of River, Wave, and Tidal Processes Than Is Indicated by External Shape. *J. Sediment. Res.* **2007**, *77*, 284–302. [CrossRef]

91. Miall, A.D. Architectural-Element Analysis: A New Method of Facies Analysis Applied to Fluvial Deposits. *Earth-Sci. Rev.* **1985**, *22*, 261–308. [CrossRef]
92. Leckie, D.A.; Walker, R.G. Storm and tide dominated shorelines in Late Cretaceous Moosebar-Lower Gates Interval—Outcrop equivalents of deep basin gas traps in western Canada. *Am. Assoc. Pet. Geol.* **1982**, *66*, 138–157.
93. De Raaf, J.F.M.; Boersma, J.R.; Van Gelder, A. Wave generated structures and sequences from a shallow marine succession, Lower Carboniferous, County Cork, Ireland. *Sedimentology* **1977**, *4*, 1–52.
94. Dumas, S.; Arnott, R.W.C. Origin of hummocky and swaley crossstratification: The controlling influence of unidirectional current strength and aggradation. *Geology* **2006**, *34*, 1073–1076. [CrossRef]
95. Pemberton, G.S.; Spila, M.; Pulham, A.J.; Saunders, T.; MacEachern, J.A.; Robbins, D.; Sinclair, I.K. *Ichnology and Sedimentology of Shallow Marine to Marginal Marine Systems: Ben Nevis and Avalon Reservoirs, Jeanne d'Arc Basin*; Short Course Notes 15; Geological Association of Canada: St. John's, NL, Canada, 2002; p. 343.
96. MacEachern, J.A.; Bann, K.L. The role of ichnology in refining shallow marine facies models. In *Recent Advances in Models of Siliciclastic ShallowMarine Stratigraphy*; Hampson, G.J., Steel, R.J., Burgess, P.M., Dalrymple, R.W., Eds.; SEPM: Tulsa, OK, USA, 2008; Volume 90, pp. 73–116.
97. Eide, C.H.; Howell, J.A.; Buckley, S.J.; Martinius, A.W.; Oftedal, B.T.; Henstra, G.A. Facies model for a coarse-grained, tide-influenced delta: Gule Horn Formation (Early Jurassic), Jameson Land, Greenland. *Sedimentology* **2016**, *63*, 1474–1506. [CrossRef]
98. Bhattacharya, J.P.; MacEachern, J.A. Hyperpycnal rivers and prodeltaic shelves in the Cretaceous seaway of North America. *J. Sediment. Res.* **2009**, *79*, 184–209. [CrossRef]
99. Nichols, G. *Sedimentology and Stratigraphy*; Blackwell Science Ltd.: London, UK, 2009; p. 335.
100. Bowman, A.P.; Johnson, H.D. Storm-dominated shelf-edge delta successions in a high accommodation setting: The palaeo-Orinoco Delta (Mayaro Formation), Columbus Basin, South-East Trinidad. *Sedimentology* **2013**, *61*, 792–835. [CrossRef]
101. Olariu, C.; Bhattacharya, J. Terminal Distributary Channels and Delta Front Architecture of River-Dominated Delta Systems. *J. Sediment. Res.* **2006**, *76*, 212–233. [CrossRef]
102. Deveugle, P.E.K.; Jackson, M.D.; Hampson, G.J.; Farrell, M.E.; Sprague, A.R.; Stewart, J.; Calvert, C.S. Characterization of stratigraphic architecture and its impact on fluid flow in a fluvial-dominated deltaic reservoir analog: Upper Cretaceous Ferron Sandstone Member, Utah. *AAPG Bull.* **2011**, *95*, 693–727. [CrossRef]
103. Tänavsuu-Milkeviciene, K.; Plink-Björklund, P. Recognizing tide-dominated versus tide-influenced deltas: Middle Devonian strata of the Baltic Basin. *J. Sediment. Res.* **2009**, *79*, 887–905. [CrossRef]
104. Goodbred, S.L.J.R.; Saito, Y. Tide-dominated deltas. In *Principles of Tidal Sedimentology*; Davis, R.A., Dalrymple, R.W., Eds.; Springer: Berlin/Heidelberg, Germany, 2012; pp. 129–149.
105. Cattaneo, A.; Steel, R.J. Transgressive deposits: A review of their variability. *Earth Sci. Rev.* **2003**, *62*, 187–228. [CrossRef]
106. Catuneanu, O.; Galloway, W.E.; Kendall, C.G.S.C.; Miall, A.D.; Posamentier, H.W.; Strasser, A.; Tucker, M.E. Sequence stratigraphy: Methodology and nomenclature. *Newsl. Stratigr.* **2011**, *44*, 173–245. [CrossRef]
107. Zecchin, M.; Catuneanu, O. High-resolution sequence stratigraphy of clastic shelves I: Units and bounding surfaces. *Mar. Pet. Geol.* **2013**, *39*, 1–25. [CrossRef]
108. Zecchin, M.; Catuneanu, O. High-resolution sequence stratigraphy of clastic shelves III: Applications to reservoir geology. *Mar. Pet. Geol.* **2015**, *62*, 161–175. [CrossRef]
109. Maravelis, A.G.; Catuneanu, O.; Nordsvan, A.; Landenberger, B.; Zelilidis, A. Interplay of tectonism and eustasy during the Early Permian icehouse: Southern Sydney Basin, southeast Australia. *Geol. J.* **2018**, *53*, 1372–1403. [CrossRef]
110. Catuneanu, O. Model-independent sequence stratigraphy. *Earth-Sci. Rev.* **2019**, *188*, 312–388. [CrossRef]
111. Willis, B.J.; Gabel, S.L. Formation of deep incisions into tide-dominated river deltas: Implications for the stratigraphy of the Sego Sandstone, Book Cliffs, Utah, USA. *J. Sediment. Res.* **2003**, *73*, 246–263. [CrossRef]
112. Catuneanu, O.; Zecchin, M. Parasequences: Allostratigraphic misfits in sequence stratigraphy. *Earth-Sci. Rev.* **2020**. [CrossRef]
113. Catuneanu, O. *Principles of Sequence Stratigraphy*; Elsevier: Amsterdam, The Netherlands, 2006; p. 375.
114. Conaghan, P.J.; Jones, J.G.; Mcdonnell, K.L.; Rouce, K. A dynamic fluvial model for the Sydney Basin. *J. Geol. Soc. Aust.* **1982**, *29*, 55–70. [CrossRef]